Government of Western Australia

REPORT 110

Department of
Mines and Petroleum

TEMPORAL AND HAFNIUM ISOTOPIC EVOLUTION OF THE GLENBURGH TERRANE BASEMENT: AN EXOTIC CRUSTAL FRAGMENT IN THE CAPRICORN OROGEN

by SP Johnson, S Sheppard, MTD Wingate, CL Kirkland, and EA Belousova

Geological Survey of Western Australia

Government of **Western Australia**
Department of **Mines and Petroleum**

REPORT 110

TEMPORAL AND HAFNIUM ISOTOPIC EVOLUTION OF THE GLENBURGH TERRANE BASEMENT: AN EXOTIC CRUSTAL FRAGMENT IN THE CAPRICORN OROGEN

by
SP Johnson, S Sheppard, MTD Wingate, CL Kirkland, and EA Belousova[1]

[1] **ARC National Key Centre for Geochemical Evolution and Metallogeny of Continents (GEMOC), Department of Earth and Planetary Sciences, Macquarie University, Sydney, 2109, New South Wales**

Perth 2011

Geological Survey of Western Australia

MINISTER FOR MINES AND PETROLEUM
Hon. Norman Moore MLC

DIRECTOR GENERAL, DEPARTMENT OF MINES AND PETROLEUM
Richard Sellers

EXECUTIVE DIRECTOR, GEOLOGICAL SURVEY OF WESTERN AUSTRALIA
Rick Rogerson

REFERENCE
The recommended reference for this publication is:
Johnson, SP, Sheppard, S, Wingate, MTD, Kirkland, CL and Belousova, EA 2011, Temporal and hafnium isotopic evolution of the Glenburgh Terrane basement: an exotic crustal fragment in the Capricorn Orogen: Geological Survey of Western Australia, Report 110, 27p.

National Library of Australia Cataloguing-in-Publication entry:

Author:	**Johnson, SP (et al.)**
Title:	**Temporal and hafnium isotopic evolution of the Glenburgh Terrane basement: an exotic crustal fragment in the Capricorn Orogen**
ISBN:	**978-1-74168-354-7 (pdf)**
Subjects:	**Geology, Structural — Western Australia — Gascoyne River Region.**
Other Authors/Contributors:	**Johnson, SP** **Geological Survey of Western Australia.** **Western Australia. Dept. of Mines and Petroleum.**
Series:	**Report (Geological Survey of Western Australia; 110.**
Dewey Decimal Classification:	**551.82099413**

ISSN 0508–4741

Grid references in this publication refer to the Geocentric Datum of Australia 1994 (GDA94). Locations mentioned in the text are referenced using Map Grid Australia (MGA) coordinates, Zone 50. All locations are quoted to at least the nearest 100 m.

U–Pb measurements were conducted using the SHRIMP II ion microprobes at the John de Laeter Centre of Mass Spectrometry at Curtin University of Technology in Perth, Australia. Lu–Hf measurements were conducted using LA-ICPMS at the ARC National Key Centre for Geochemical Evolution and Metallogeny of Continents (GEMOC) based in the Department of Earth and Planetary Sciences at Macquarie University, Australia. Geochemical and isotopic analyses in this publication were funded in part by the Western Australian government Exploration Incentive Scheme (EIS).

Copy editor: SK Martin
Cartography: SN Dowsett
Desktop publishing: KS Noonan

Published 2011 by Geological Survey of Western Australia
This Report is published in digital format (PDF) and is available online at <http://www.dmp.wa.gov.au/GSWApublications>.

Further details of geological publications and maps produced by the Geological Survey of Western Australia are available from:
Information Centre
Department of Mines and Petroleum
100 Plain Street
EAST PERTH, WESTERN AUSTRALIA 6004
Telephone: +61 8 9222 3459 Facsimile: +61 8 9222 3444
<http://www.dmp.wa.gov.au/GSWApublications>

Cover photograph:
Complexly folded, pegmatite-banded mesocratic gneiss of the Halfway Gneiss from Injinu Spring on Pink Hills (MGA 452716E 7261127N). Hammer is 30cm in length.

Contents

Appendix

Figures

Tables

Temporal and hafnium isotopic evolution of the Glenburgh Terrane basement: an exotic crustal fragment in the Capricorn Orogen

by

SP Johnson, S Sheppard, MTD Wingate, CL Kirkland, and EA Belousova[1]

Abstract

The Glenburgh Terrane of the Paleoproterozoic Capricorn Orogen is a wedge-shaped tract of Archean to Paleoproterozoic rocks, lying between the Archean Yilgarn and Pilbara Cratons. The terrane contains a basement of granitic gneisses, termed the Halfway Gneiss, the protoliths to which have crystallization ages between 2555 and 2430 Ma. Inherited zircons within the gneisses are as old as 3447 Ma, and together with hafnium model ages ($T_{DM}^{crustal}$) for both magmatic and inherited zircons as old as 3700 Ma, indicate an ancient Archean source. The Hf-isotopic compositions of numerous magmatic and inherited zircons indicate a major period of crustal growth between 2730 and 2600 Ma, possibly in a continental-margin arc. However, much of the Halfway Gneiss formed between 2600 and 2430 Ma, mainly by the reworking of 2730–2600 Ma crust. Comparison of the crystallization history and isotopic evolution of the Halfway Gneiss with both the Pilbara and Yilgarn Cratons demonstrates that the Glenburgh Terrane is exotic to both these cratons. The tectonomagmatic history of the Halfway Gneiss indicates a multi-phase assembly for the Western Australian Craton.

KEYWORDS: Gascoyne Province, Glenburgh Terrane, hafnium isotopes, West Australian Craton, geochronology, zircon

Introduction

The Capricorn Orogen in central Western Australia records the juxtaposition of the Archean Yilgarn and Pilbara Cratons to form the West Australian Craton (Fig. 1; Tyler and Thorne, 1990; Cawood and Tyler, 2004). The orogen includes the deformed craton margins, plus a wedge of granitic gneisses and metasedimentary rocks in the Gascoyne Province termed the Glenburgh Terrane. The Glenburgh Terrane comprises: a basement of granitic gneisses (the Halfway Gneiss) with ages between 2555 and 2430 Ma; an overlying package of continent-derived siliciclastic metasedimentary rocks (Moogie Metamorphics); a c. 2000 Ma belt of metagranitic rocks (Dalgaringa Supersuite) interpreted to have formed in a continental-margin volcanic arc (Sheppard et al., 2004; Johnson et al., 2010b); and arc-related metasedimentary rocks (Camel Hills Metamorphics) in tectonic contact with both the Dalgaringa Supersuite and the deformed northern margin of the Yilgarn Craton.

[1] ARC National Key Centre for Geochemical Evolution and Metallogeny of Continents (GEMOC), Department of Earth and Planetary Sciences, Macquarie University, Sydney, 2109, New South Wales

Based on lithological similarities, both Williams (1986) and Myers (1990) considered the Halfway Gneiss and elements of the Glenburgh Terrane to represent a pervasively reworked part of the Yilgarn Craton. Williams (1986) considered the entire Gascoyne Province to be underlain by Archean crust that had undergone pervasive Paleoproterozoic intracontinental deformation and metamorphism. In contrast, Myers (1990) and Tyler and Thorne (1990) proposed a single collision between the Pilbara and Yilgarn Cratons during the Paleoproterozoic Capricorn Orogeny, with the suture located somewhere to the north of the Minnie Creek batholith (i.e. north of the exposed Halfway Gneiss). Subsequent mapping in the southern part of the province led to the recognition of a suite of meta-igneous rocks (Dalgaringa Supersuite) that have geochemical and isotopic signatures similar to those within present-day continental margin arcs (Sheppard et al., 2004).

Two lines of evidence led Sheppard et al. (2004) and Occhipinti et al. (2004) to propose a second suture located along the Errabiddy Shear Zone (Figs 1 and 2). First, the Dalgaringa Supersuite only occurs along the southern margin of the Glenburgh Terrane, rather than within the Yilgarn Craton. Second, geochronological studies show that the bulk of the Halfway Gneiss has crystallization

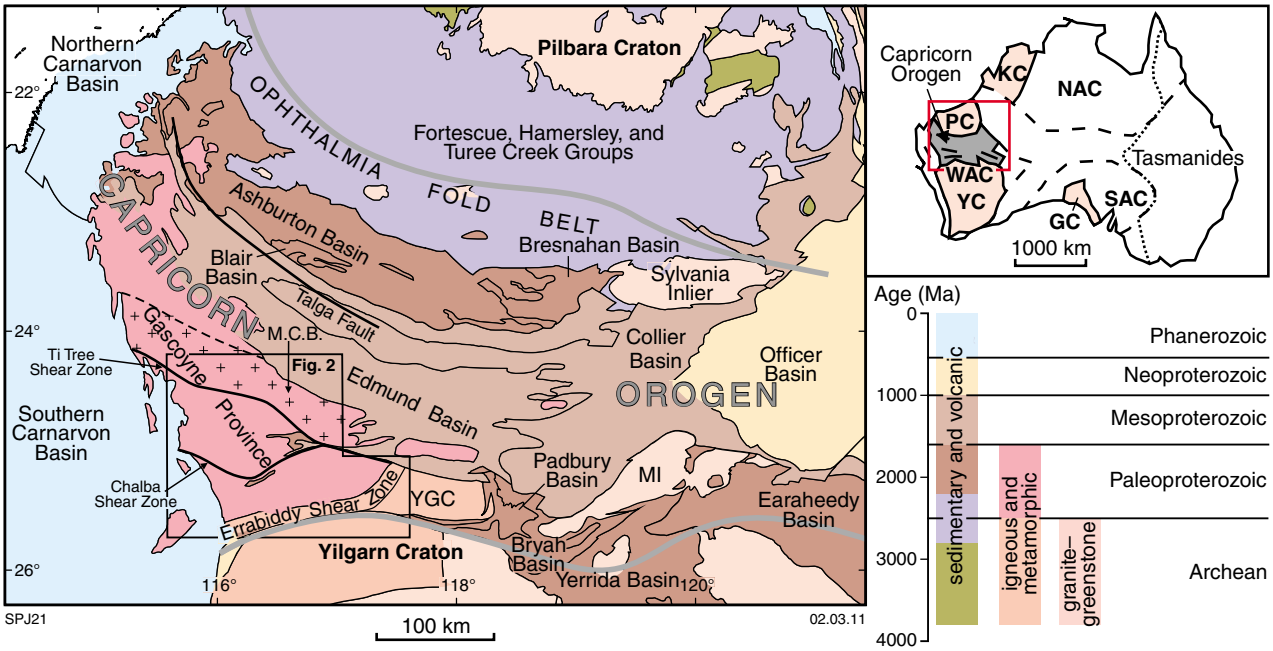

Figure 1. Elements of the Capricorn Orogen and surrounding cratons and basins; modified from Sheppard et al. (2010a) and Martin and Thorne (2004). Inset shows location of the Capricorn Orogen, Paleoproterozoic (NAC — North Australian Craton; SAC — South Australian Craton; WAC — West Australian Craton; KC — Kimberley Craton), and Archean (YC — Yilgarn Craton; PC — Pilbara Craton; GC — Gawler Craton) crustal elements. Other abbreviations: YGC — Yarlarweelor Gneiss Complex; MCB — Minnie Creek batholith; MI — Marymia Inlier; modified from Myers et al. (1996).

ages between 2555 and 2430 Ma (Kinny et al., 2004; Geological Survey of Western Australia, 2009); there are no known rocks of this age in the Yilgarn Craton. Furthermore, these ages appear to only partly overlap with ages of magmatic activity associated with deposition of the Hamersley, Fortescue, and Turee Creek Groups on the Pilbara Craton margin (Thorne and Seymour, 1991; Barley et al., 1997; Pickard, 2002; Rasmussen et al., 2005a). These results imply that the Glenburgh Terrane is exotic to both the Pilbara and Yilgarn Cratons. The presence of two sutures is supported by a recent magnetotelluric (MT) survey (Selway, 2008; Selway et al., 2009) that showed that the Glenburgh Terrane has a distinctly different electrical character to that of either of the bounding cratons (Fig. 3).

In light of this geochemical, geophysical, and geochronological information, various authors proposed a two-stage collisional model for the assembly of the West Australian Craton (Occhipinti et al., 2004; Martin and Morris, 2010; Sheppard et al., 2010a; Johnson et al., 2010b; Sheppard et al., 2010b). In the first stage, the Glenburgh Terrane collided with, or accreted to, the Pilbara Craton during the 2215–2145 Ma Ophthalmian Orogeny (Blake and Barley, 1992; Occhipinti et al., 2004; Martin and Morris, 2010). This suture is buried by the upper Wyloo Group (including the Ashburton Formation), but is interpreted using geophysical data (Abdulah, 2007; Selway, 2008; Selway et al., 2009) to roughly coincide with the Talga Fault (Figs 1 and 3; Selway, 2008; Selway et al., 2009; Sheppard et al., 2010a; Sheppard et al., 2010b), a major structure that intermittently controlled deposition within the overlying Mesoproterozoic Edmund Basin (Martin and Thorne, 2004; Martin et al., 2008). The second phase consisted of a combined Pilbara Craton – Glenburgh Terrane (the informally named 'Pilboyne Craton' of Sheppard (2005)) colliding with the Yilgarn Craton along the Errabiddy Shear Zone during the 2005–1950 Ma Glenburgh Orogeny (Occhipinti et al., 2004; Sheppard et al., 2010a; Johnson et al., 2010b; Sheppard et al., 2010b). It is during the Glenburgh Orogeny that the Glenburgh Terrane attained its principal structural grain, with many of the granitic and sedimentary rocks acquiring high-grade gneissic fabrics and metamorphic assemblages (Occhipinti et al., 2004; Johnson et al., 2010b). However, the tectonomagmatic history of the Glenburgh Terrane is poorly constrained prior to its c. 2200 Ma amalgamation with the Pilbara Craton.

This Report presents a variety of geological information on the oldest part of the Glenburgh Terrane, the Halfway Gneiss, in an effort to define the gneiss' magmatic and tectonic history. Most of this information is freely available on DVD or downloadable from the Geological Survey of Western Australia (GSWA) data centre, but has never been integrated in a coherent format. These data include U–Pb dating of magmatic and xenocrystic zircons using the sensitive high-resolution ion microprobe (SHRIMP), and whole-rock major, trace, and rare-earth element data (GSWA GeoChem Extract online). This information is complemented by newly acquired hafnium isotopic data, obtained by Laser Ablation Inductively Coupled Mass Spectrometry (LA-ICP-MS) for dated magmatic and xenocrystic zircons. The combined dataset provides constraints on the tectonomagmatic history of the Glenburgh Terrane prior to its collision with the Pilbara and Yilgarn Cratons.

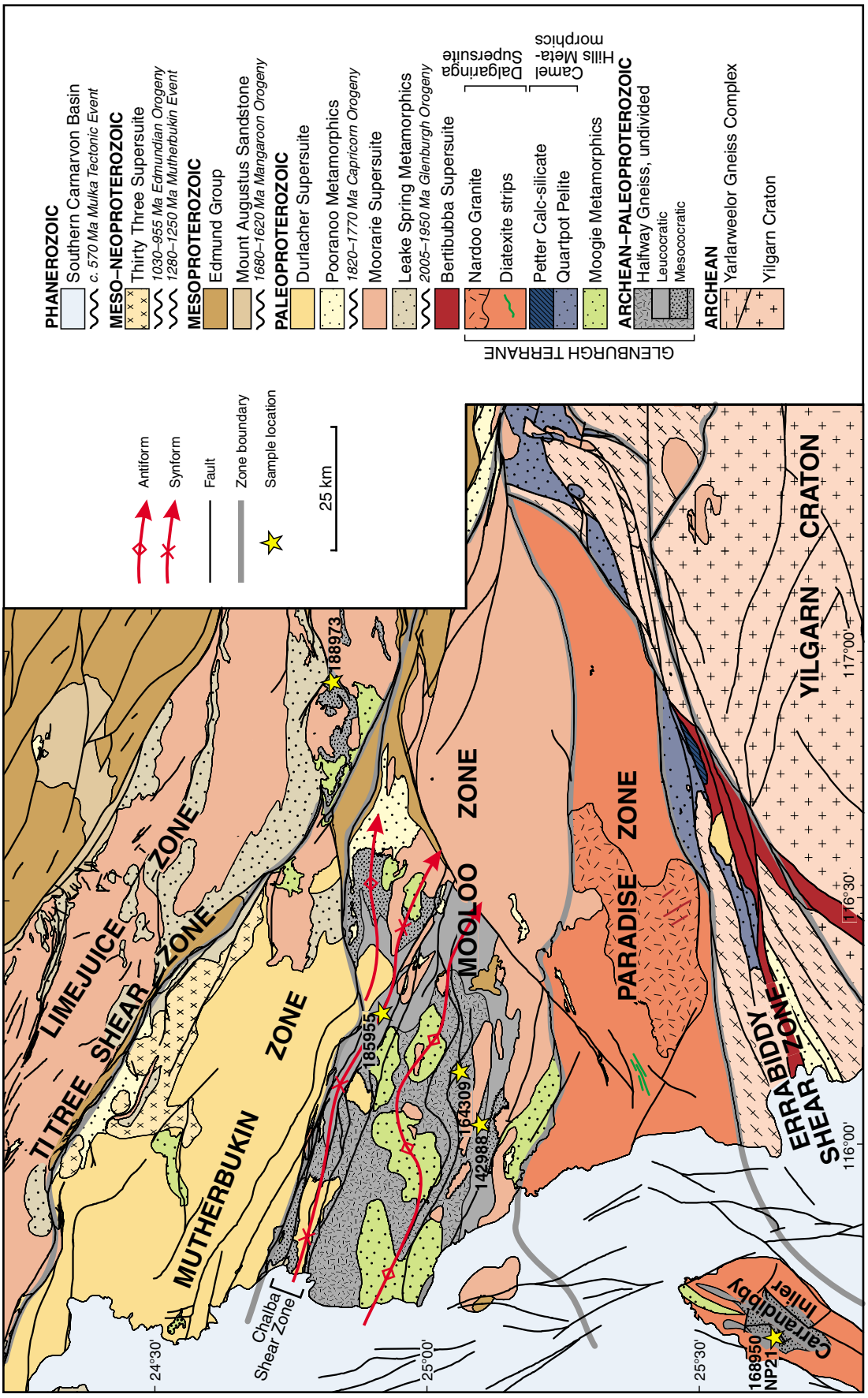

Figure 2. Simplified geological map of the southern Gascoyne Province, showing division of the region into various structural–metamorphic zones (after Sheppard et al., 2010b). Locations of dated samples are shown by yellow stars accompanied by their GSWA sample number. Sample NP21 was dated by Kinny et al. (2004).

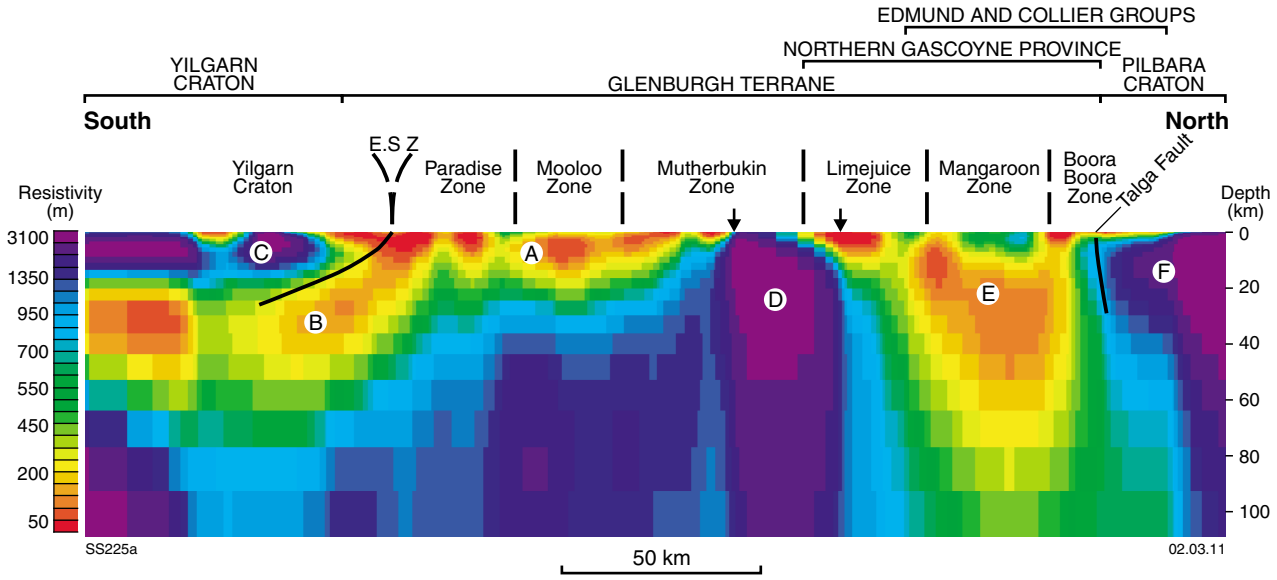

Figure 3. 2D model of magnetotelluric data collected from a traverse across the Gascoyne Province (Selway, 2008; Selway et al., 2009). The low resistivity features (A, B, and E) are interpreted to represent the Glenburgh Terrane. Note that the Glenburgh Terrane dips southward at B, under the Yilgarn Craton at the location of the Errabiddy Shear Zone (E.S.Z). Note that this geometry contrasts with evidence that subduction was to the north under the Glenburgh Terrane prior to the collision of the Yilgarn Craton and Glenburgh Terrane during the 2005–1950 Ma Glenburgh Orogeny. The Yilgarn (C) and Pilbara (F) Cratons are regions of high resistivity. The apparent highly resistive area at D (between the two arrows) is an artefact, resulting from data loss from stations in this area. For more details on the modelling parameters and interpretation of data, see Selway (2008) and Selway et al. (2009).

The Gascoyne Province

The Gascoyne Province* comprises granitic and medium- to high-grade metamorphic rocks at the western end of the Capricorn Orogen (Figs 1 and 2). The province is overlain by sedimentary rocks of the Mesoproterozoic Edmund and Collier Basins to the east, and by sedimentary rocks of the Phanerozoic Carnarvon Basin to the west. The southern margin of the province is bounded by the Errabiddy Shear Zone, and to the north, Gascoyne Province metasedimentary rocks are interpreted to pass with decreasing metamorphic grade into low-grade metasedimentary rocks of the Ashburton Basin, in particular the Ashburton Formation (Williams, 1986).

The Gascoyne Province has been divided up into several east–southeasterly trending structural and metamorphic domains, or zones (Figs 2 and 4; Sheppard et al., 2010b), each of which is characterized by a unique geological history. These crustal zones are bounded by major faults or shear zones, but none are interpreted to be exotic terranes. Rather, each zone reflects a different response to the multiple reworking events that distinguish the Gascoyne Province from other units in the Capricorn Orogen (Sheppard et al., 2010b).

* Use of the term 'Gascoyne Complex' has been discontinued, because 'complex' is a lithostratigraphic term, and the term 'Gascoyne Province' is reinstated. The following definition of a 'province' is taken from GSWA Memoir 2: 'An area of the earth's crust in which the rocks have some geological character, or combination of characters, in common; these are usually either age, metamorphic grade, structural style or type of mineralization' (Trendall, 1975, p. 30).

The Glenburgh Terrane

The oldest crust in the Gascoyne Province is the Glenburgh Terrane, which is exposed only within the southern part of the province, from the Paradise Zone through to the Limejuice Zone (Figs 2 and 4). The southern boundary of the Glenburgh Terrane is marked by the Errabiddy Shear Zone, a high-strain zone up to 25 km wide that contains imbricate slices of reworked Yilgarn Craton (termed the Yarlarweelor Gneiss Complex; Figs 1 and 2). The northern margin of the terrane is not exposed, but interpreted on the basis of a recent MT survey to coincide roughly with the Talga Fault (Fig. 3; Selway, 2008; Selway et al., 2009), implying that the Glenburgh Terrane also forms basement to the northern part of the Gascoyne Province. Structures and metamorphic mineral assemblages related to the collision of the Glenburgh Terrane with the Pilbara Craton are absent at the surface due to younger sedimentary cover, and overprinting by high-grade reworking events in the northern Gascoyne Province.

The oldest rocks in the Glenburgh Terrane are heterogeneous granitic gneisses known as the Halfway Gneiss. The igneous protoliths to these gneisses have crystallization ages between 2555 and 2430 Ma (Fig. 4; Kinny et al., 2004; Geological Survey of Western Australia, 2009). Felsic components dated at c. 2000 Ma, previously thought to be integral components of the gneiss (Occhipinti and Sheppard, 2001), are now interpreted as parts of the Dalgaringa Supersuite emplaced into the gneiss during subduction prior to the Glenburgh Orogeny (Sheppard et al., 2010b). The Halfway Gneiss also contains numerous inherited zircons as old as c. 3450 Ma, indicating that the gneiss protoliths were either sourced

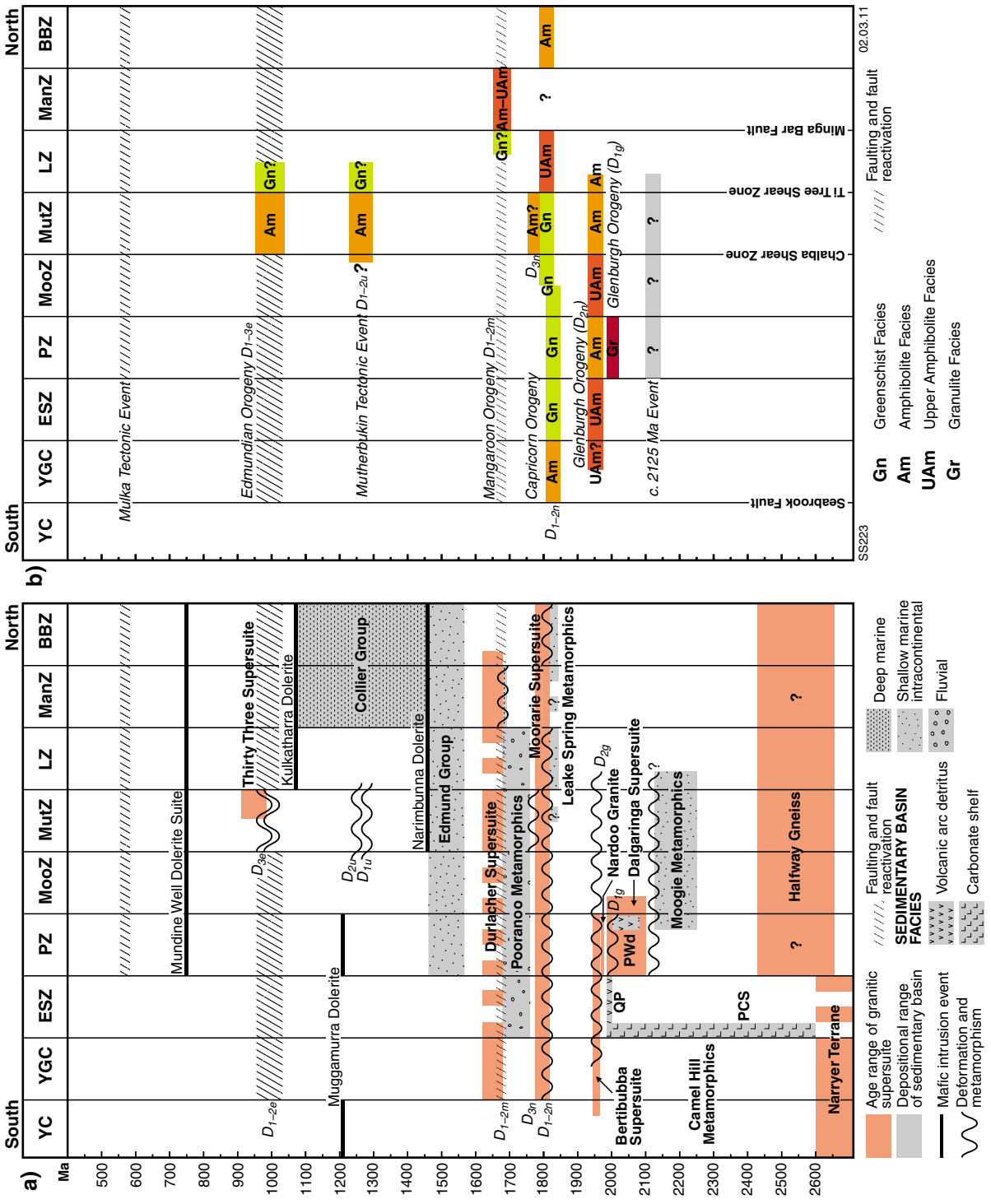

Figure 4. **Time–space plot for the Gascoyne Province. Zone boundary abbreviations: BBZ — Boora Boora Zone; ESZ — Errabiddy Shear Zone; LZ — Limejuice Zone; ManZ — Mangaroon Zone; MooZ — Mooloo Zone; MutZ — Mutherbukin Zone; PZ — Paradise Zone; YC — Yilgarn Craton; YGC — Yarlarweelor Gneiss Complex. Abbreviations in time–space plot: PCS — Petter Calc-silicate; QP — Quartpot Pelite; PWd — Paradise Well diatexite.**

from, or interacted with, much older rocks during their formation. The gneisses range in composition from tonalite to monzogranite, and are intruded by several generations of centimetre- to metre-scale pegmatite dykes and/or leucocratic granite veins. These leucocratic dykes and veins partly define the gneissic fabrics, which locally show complex folding and refolding patterns (Occhipinti et al., 2004; Johnson et al., 2010b). The gneissic fabrics, and the folds and refolds, are interpreted to have developed during the collisional phase of the Glenburgh Orogeny (D_{2g}) at 1965–1950 Ma (Johnson et al., 2010b).

The Halfway Gneiss is in tectonic contact with, and locally unconformably overlain by, siliciclastic metasedimentary rocks of the Moogie Metamorphics. This metasedimentary package is dominated by psammitic schist (the Mumba Psammite), but also includes pelitic schist, quartzite, calc-silicate, and marble. Based on the ages of the youngest detrital zircons extracted from the Mumba Psammite, protoliths to the Moogie Metamorphics were deposited after c. 2240 Ma (Johnson et al., 2010b). The age distribution of the detrital zircons also indicates that they were derived partly from the underlying Halfway Gneiss, and may have been deposited either as a foreland basin to the 2215–2145 Ma Ophthalmian Orogeny, or within a retro-arc basin (Johnson et al., 2010b). The local presence of c. 2125 Ma metamorphic zircons and monazites within the Mumba Psammite suggest that parts of this package, and presumably also the underlying Halfway Gneiss, were subjected to a medium-grade metamorphic/hydrothermal event at this time (Johnson et al., 2010b). If correct, this also provides a minimum age for deposition of the sedimentary package.

The southern margin of the Glenburgh Terrane contains a variably deformed and metamorphosed granitic batholith dated at 2005–1970 Ma (Sheppard et al., 2004; Geological Survey of Western Australia, 2009; Johnson et al., 2010b). This belt of intermediate to felsic plutonic rocks, known as the Dalgaringa Supersuite (Fig. 4), has Andean-type subduction zone geochemical and isotopic characteristics (Sheppard et al., 2004). The batholith is thought to have developed along the southern margin of the Glenburgh Terrane, prior to its collision with the passive margin of the Yilgarn Craton during the Glenburgh Orogeny (Sheppard et al., 2004). Most older plutonic rocks in the supersuite have been strongly deformed, and locally contain decametre-scale strips and lenses of granulite-facies pelitic diatexite. High-grade deformation and metamorphism appears to have been synchronous with the intrusion of the gneiss' protoliths at 2005–1985 Ma. SHRIMP U–Pb dating of metamorphic zircons from a pelitic diatexite lens confirms this interpretation (Johnson et al., 2010b). This tectono-metamorphic event is considerably older than the high-grade event associated with the collision between the Glenburgh Terrane and the Yilgarn Craton (i.e. D_{2g} at 1965–1950 Ma), and is interpreted to record the construction of the magmatic arc in the middle to lower crust (Johnson et al., 2010b). This event (D_{1g}) is recorded only within units of the Dalgaringa Supersuite (Fig. 4).

The Quartpot Pelite, part of the Camel Hills Metamorphics, includes pelitic to semipelitic schist and gneiss that occur as isolated, fault-bounded lenses within the Errabiddy Shear Zone (Figs 2 and 4). SHRIMP dating of detrital zircons from this unit indicates that the package was deposited sometime after c. 2000 Ma, but prior to growth of new zircon during high-grade metamorphism (D_{2g}) at c. 1965 Ma (Fig. 4). Deposition appears to have been synchronous with the older part of the Glenburgh Orogeny (D_{1g}) at 2005–1985 Ma. The age range and $^{177}Hf/^{176}Hf$ isotopic compositions of the detrital zircons suggest that the Quartpot Pelite was derived through erosion of an older (2080–2000 Ma), currently unexposed, part of the Dalgaringa arc.

High-grade metamorphism, the melting of pelitic to semipelitic lithologies within the Moogie and Camel Hills Metamorphics, and the tectonic interleaving of lithologies, occurred during the collision of the Glenburgh Terrane with the Yilgarn Craton (i.e. D_{2g} of the Glenburgh Orogeny; Johnson et al., 2010b). This event was accompanied by the intrusion of the granitic 1965–1945 Ma Bertibubba Supersuite, which is the first magmatic element common to the northern margin of the Yilgarn Craton, the Yarlarweelor Gneiss Complex, the Errabiddy Shear Zone, and the Glenburgh Terrane (Figs 2 and 4).

The Halfway Gneiss: distribution and lithologies

The Halfway Gneiss consists of interlayered granitic gneisses, which have been heterogeneously deformed and metamorphosed to at least amphibolite facies. These gneisses occur within the Paradise, Mooloo, and Limejuice Zones (Fig. 2). The rock types include interlayered leucocratic granitic gneiss and foliated leucocratic metagranite, mesocratic granitic gneiss, augen gneiss, pegmatite-banded tonalitic and granodioritic gneiss, pale-grey granitic gneiss, gneissic to foliated porphyritic metagranodiorite, foliated metagranite, and metapegmatite. There are no sharp boundaries between the various rock types, as they are interleaved at both mesoscopic and megascopic scales, but two mappable units (at 1:100 000 scale) have been recognized: (1) mesocratic granitic gneiss, and (2) leucocratic granitic gneiss and foliated metagranite. The mapped boundaries of the leucocratic and mesocratic gneisses define areas of dominance of one gneiss type over the other. In areas where neither mesocratic nor leucocratic gneiss dominates, the gneiss has been mapped simply as an undivided unit. However, within this undivided unit there are discrete pale-grey granitic gneisses not present within either the leucocratic or mesocratic portions.

Undivided Halfway Gneiss

Undivided Halfway Gneiss includes pale-grey granitic gneiss, augen gneiss, pegmatite-banded mesocratic gneiss, and a series of leucocratic gneisses. This undivided unit makes up the majority of the Halfway Gneiss in the southern Glenburgh Terrane (Fig. 2). The unit is developed in a belt about 50 km long and 25 km wide, forming the

core of a regional-scale (25 km wavelength), tight to isoclinal, steeply southeast-plunging fold in the Mooloo Zone (Fig. 2; Occhipinti and Sheppard, 2000; Sheppard et al., 2008; GSWA, unpublished data). The unit also occurs within the Limejuice Zone on the northern side of the Ti Tree Shear Zone, where it is either intercalated with younger schists and granites, or overlain by sedimentary rocks of the Mount Augustus Sandstone and Yilgatherra Formation of the Edmund Group (Thorne et al., 2010; Johnson et al., 2010a). Undivided gneiss is also present in the Carrandibby Inlier in the Paradise Zone, where it is intruded by, and interleaved with, banded gneisses of the 2005–1970 Ma Dalgaringa Supersuite (Fig. 2; GSWA, unpublished data).

Pale-grey granitic gneiss is the only unit unique to the undivided Halfway Gneiss, being abundant in the southern and southeastern parts of the map area (Occhipinti and Sheppard, 2000). This gneiss unit generally forms metre-scale lenses within the more dominant pegmatite-banded tonalitic to granodioritic gneiss. It is typically fine to medium grained, and is weakly to moderately pegmatite banded. In lower-strain domains, the granitic gneiss consists of medium-grained, equigranular or weakly porphyritic, biotite metagranodiorite and quartz-rich leucocratic metatonalite, and contains numerous discontinuous leucocratic veins. The gneiss consists of plagioclase–quartz–biotite–K-feldspar–epidote, with accessory zircon and titanite. Owing to pervasive pegmatite and leucocratic veining, this gneiss has not previously been sampled for geochronology or geochemistry. The bulk of the undivided Halfway Gneiss comprises pegmatite-banded mesocratic gneiss and leucocratic gneisses. Both of these lithologies are described in the following sections.

Three samples of undivided Halfway Gneiss were collected for geochronology, geochemistry, and isotope analyses (sample details are in Table 1). Sample GSWA 164309 is a foliated, homogenous, porphyritic biotite metagranodiorite free of pegmatitic and leucocratic veins. Sample GSWA 168950 is a fine- to medium-grained, weakly porphyritic biotite granodiorite gneiss. Kinny et al. (2004) reported additional geochronological data for a pegmatite-banded granodiorite orthogneiss collected from the same locality as GSWA 168950.

Mesocratic Halfway Gneiss

Mesocratic gneiss constitutes a significant component of the Halfway Gneiss, forming numerous irregularly shaped bodies at outcrop scale, which are generally too small to separate from the undivided Halfway Gneiss. However, mesocratic gneiss does form mappable units. In the southern part of the Mooloo Zone, the gneiss forms an elongate, 1 km wide, 8 km long body along the southern limb of a regional-scale, tight to isoclinal fold (Fig. 2; Occhipinti and Sheppard, 2000; GSWA, unpublished data). Farther north in the central and northern parts of the Mooloo Zone, the gneiss forms a 5 km wide, 50 km long, southeast-trending belt that defines the northern limb of the regional-scale fold (Fig. 2; Sheppard et al., 2008; GSWA, unpublished data). Further to the west, the mesocratic unit is found on both sides of the Ti Tree Shear Zone, where it is interleaved with psammitic schist and quartzite of the Moogie Metamorphics and intruded by stocks and sheets of granite belonging to the 1820–1775 Ma Moorarie Supersuite, or occurs as elongate rafts within these younger granitic bodies (Fig. 2; Thorne et al., 2010; Johnson et al., 2010a).

Mesocratic granitic gneiss is a fine- or medium-grained, pegmatite-banded, dark-grey meta-igneous rock (Fig. 5a,b). Lower-strain domains consist of foliated, fine-grained, weakly porphyritic metatonalite to metagranodiorite, and medium-grained, strongly porphyritic metatonalite (Fig. 5c). Pegmatite banding is variable across the region, with pegmatites of various generations comprising 5–30% of the gneiss. Within low-strain areas, the fine-grained metatonalite and metagranodiorite typically contain about 10% rounded plagioclase phenocrysts a few millimetres in diameter, whereas the medium-grained units contain up to 30% round, equant, or locally amoeboid, plagioclase phenocrysts about 5–20 mm in diameter. The groundmass consists of plagioclase, quartz, and biotite (15–20% of the rock), with accessory apatite and zircon. Some amoeboid textures are present in the groundmass, implying metamorphism at medium to high grade. Quartz and plagioclase commonly define a foliation. In the granodioritic parts of the gneiss, similar textures and mineral phases are present, except that K-feldspar becomes more prominent in the matrix, and can locally comprise up to 20% of the phenocrysts.

Table 1. Summary of location and age data for the U–Pb SHRIMP dated samples

Geochron ID	*Zone*	*Sample description*	*Sample locality*	*Easting*	*Northing*	*Igneous crystallization age (Ma)*
Undivided Halfway Gneiss						
164309	Mooloo	foliated porphyritic biotite granodiorite	Middle Well	413480	7225160	2555 ± 4
168950	Paradise	pegmatite-banded tonalite gneiss	Yandarra Well	360580	7165930	2518 ± 2
NP21[(a)]	Paradise	orthogneiss	Yandarra Well	360580	7165930	2508 ± 5
Mesocratic Halfway Gneiss						
142988	Mooloo	biotite tonalite	Dunnawah Bore	401300	7223420	2552 ± 4
188973	Limejuice	metagranodiorite	Mount James Homestead	491577	7251062	2429 ± 4
Leucocratic Halfway Gneiss						
185955	Mooloo	leucocratic gneiss	Wabli Creek	428780	7244930	2527 ± 9

NOTES: (a) Data from Kinny et al. (2004)

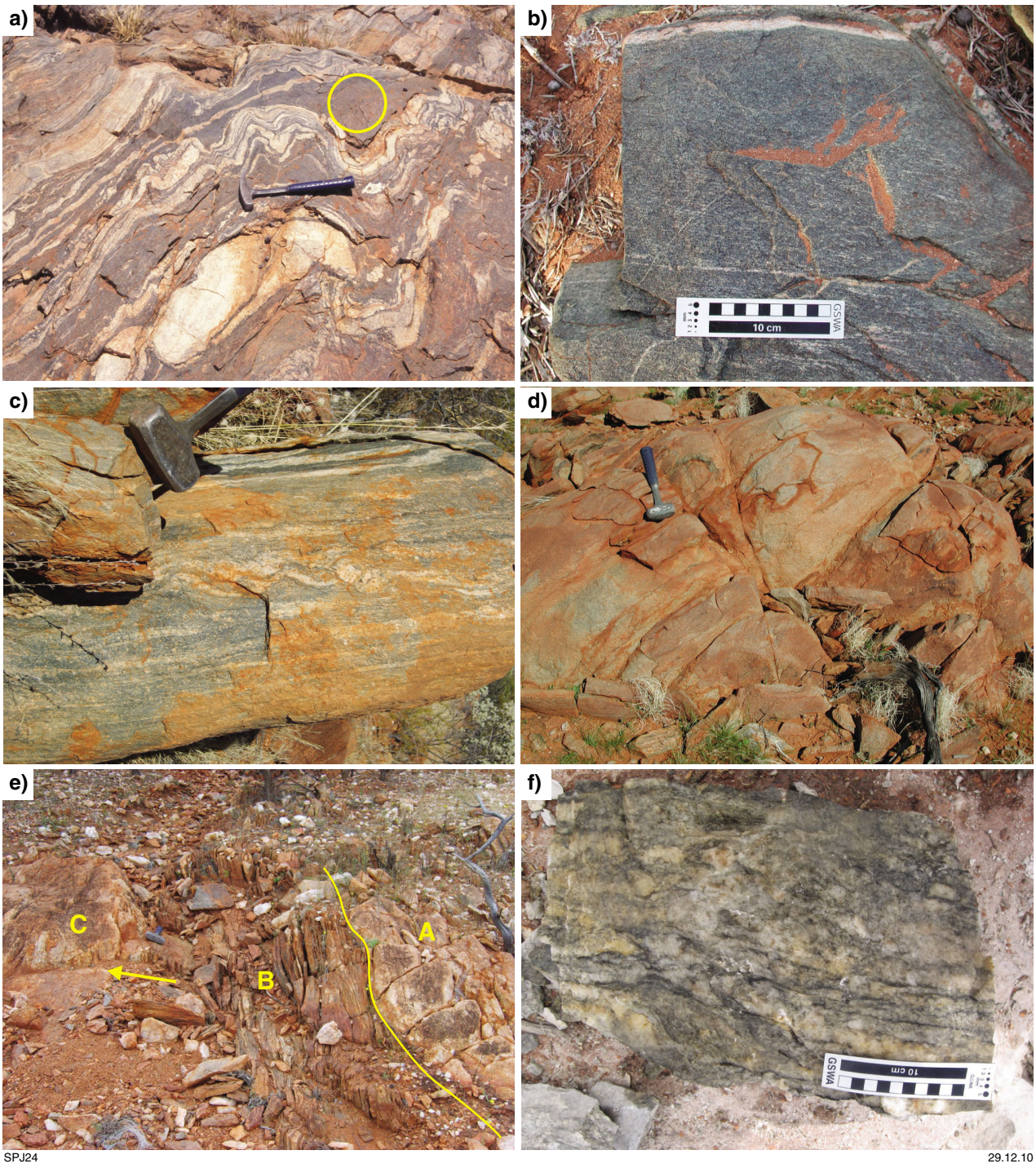

Figure 5. **Macroscopic features of the Halfway Gneiss: a) planar, pegmatite-banded tonalite gneiss, consisting of a dark, fine-grained metatonalite intruded by numerous leucocratic granitic veins. This lithology is characteristic of the mesocratic Halfway Gneiss. Circle shows the location of dated sample GSWA 142988; b) fine-grained metamafic portion of the planar, pegmatite-banded tonalite gneiss GSWA 142988. This sample (GSWA 178774) was analysed for whole-rock major, trace, and rare-earth element concentrations; c) fine-grained, pegmatite-banded granodiorite gneiss (GSWA 188973) selected for U–Pb zircon geochronology. This rock forms a minor component within the mesocratic Halfway Gneiss; d) fine- to medium-grained, biotite-poor, weakly foliated leucocratic metagranite. This lithology is representative of the leucocratic Halfway Gneiss; e) massive to weakly foliated, biotite-poor leucocratic granite (A and C) with a metre-scale band of strongly deformed biotite-rich leucocratic gneiss (B). The boundary between the gneiss and weakly foliated granite (yellow line between A and B) is sharp, although the contact of the gneiss (B) with the massive to foliated granite (C) is gradational; f) pegmatite-banded leucocratic gneiss sample GSWA 185955. Hammer in a, c–e is 30 cm long.**

Three samples of mesocratic gneiss were collected for geochronology, geochemistry, and isotope analysis (Table 1). Firstly, a sample of medium-grained biotite granodiorite gneiss (GSWA 142988; Fig. 5a) considered representative of the mesocratic gneiss portion of the undivided Halfway Gneiss unit (Occhipinti and Sheppard, 2000) was sampled. A finer grained ?tonalitic portion (Fig. 5b) of the same gneiss, which is free of leucocratic and pegmatitic veins, was collected only for geochemical analysis (GSWA 178774); although undated, this latter sample is considered to represent the most mafic part of the mesocratic gneiss. Finally, sample GSWA 188973 (Fig. 5c; Table 1) is a fine-grained pegmatite-banded ?granodiorite gneiss (Johnson et al., 2010a).

Leucocratic Halfway Gneiss

The leucocratic gneiss component of the Halfway Gneiss is present throughout all parts of the Glenburgh Terrane, but generally forms disparate outcrop-scale units that are generally too small to separate from the main, undivided gneissic unit. Larger, more continuous, mappable outcrops of leucocratic gneiss occur in the southern part of the Mooloo Zone, where it forms a 6 km wide, east-trending linear belt that defines the southern limb of a regional-scale isoclinal fold (Fig. 2; Occhipinti and Sheppard, 2000; GSWA, unpublished data). The same unit is folded around the southeast-trending, regional-scale fold hinge as a northwest-trending belt about 7 km wide (Sheppard et al., 2008; GSWA, unpublished data).

Leucocratic granitic gneiss is generally medium grained, although locally coarse grained, and contains thin, discontinuous layers of biotite that give it a flaser texture defining the foliation or gneissic layering. Biotite contents are variable, ranging from <5% to 25%, and this variation is observed on both outcrop and regional scales. The gneisses range from weakly to moderately pegmatite banded. Lower strain domains of the gneiss consist of foliated, coarse-grained porphyritic biotite granite, and minor foliated fine- to medium-grained, equigranular granite (Fig. 5d), and may contain metre- to decametre-wide inclusions of recrystallized quartzite and calc-silicate rock. Units with higher biotite contents (15–25%) become distinctly banded, and a single outcrop may consist of both strongly foliated gneiss and apparently weakly deformed, coarser grained biotite granite (Fig. 5e). Precursors to the gneiss range from granodiorite to monzogranite. The porphyritic granite contains about 10–30% round and equant, 1–3 cm long, tabular phenocrysts of microperthite in a groundmass of plagioclase, quartz, microperthite, and minor biotite, with or without muscovite. The rocks commonly exhibit micrographic and myrmekitic textures.

A single sample of biotite-rich (15–20%) monzogranite gneiss (GSWA 185955; Fig. 5f) from the northern part of the Mooloo Zone (Sheppard et al., 2008), was collected for geochronology and geochemistry (Fig. 2; Table 1).

Whole-rock geochemistry

Sampling the different end-member phases of the Halfway Gneiss is difficult because of the centimetre- to decametre-scale compositional heterogeneity. However, the few samples collected for geochronology represent fresh material free of inclusions and veins, and the geochemical analyses reported here were also limited mainly to these samples. Due to the limited number of samples, the aim is to provide only a brief description of their whole-rock major, trace, and rare-earth element (REE) abundances (Table 2), rather than attempt to define their tectonomagmatic setting.

Apart from the most mafic sample (SiO_2 content of ~48%) collected from a mesocratic gneiss (GSWA 178774), all other samples have granitic compositions with SiO_2 contents of 64–74% (Table 2). Using the three-tier classification scheme of Frost et al. (2001), granites from the undivided and mesocratic Halfway Gneiss are classified as magnesian (Fig. 6a), calc-alkalic to alkali-calcic (Fig. 6b), and are peraluminous (Fig. 6c). Irrespective of major-element composition, these granitic rocks have slightly variable total REE concentrations, but similar chondrite-normalized (Nakamura, 1974) REE patterns (Fig. 6d). The granites have negative-sloping patterns, with elevated light REE ($La_N^*/Sm_N = 3.49–5.18$), flatter heavy REE profiles ($Eu_N/Yb_N = 1.54–2.77$), and moderate Eu anomalies ($Eu/Eu^* = 0.28–0.63$).

Compared with granitic gneiss of the undivided and mesocratic Halfway Gneiss, the leucocratic monzogranite gneiss (GSWA 185955) from the leucocratic Halfway Gneiss unit is ferroan (Fig. 6a), calc-alkalic (Fig. 6b), and strongly peraluminous (Fig. 6c). The sample has lower REE concentrations (Table 2), but similar light REE ($La_N/Sm_N = 4.67$) slopes and Eu anomalies ($Eu/Eu^* = 0.63$), and a much flatter heavy REE profile than the other samples ($Eu_N/Yb_N = 1.39$; Fig. 6d).

As the fine-grained homogenous metamafic sample (GSWA 178774) is undated, its composition is difficult to place into context. However, for completeness, the sample's chemical analyses are still provided in Table 2.

Ion microprobe (SHRIMP) U–Pb geochronology

This section summarizes the U–Pb zircon geochronology of Halfway Gneiss samples. Results for two samples analysed by Nelson (2000b; 2001) and one by Kinny et al. (2004) are reinterpreted below, and additional data are described for one sample reported by Nelson (2000a).

* The subscript 'N' indicates that the trace element value has been normalized against that of chondrite (Nakamura, 1974).

Table 2. Whole rock major, trace, and rare-earth element data for the Halfway Gneiss

	Undivided Halfway Gneiss			*Mesocratic Halfway Gneiss*		*Leucocratic Halfway Gneiss*
	142988	*178774*	*168950*	*188973*	*164309*	*185955*
SiO_2	64.70	48.56	72.39	71.61	70.28	74.41
TiO_2	0.64	1.84	0.22	0.32	0.54	0.05
Al_2O_3	15.21	13.09	14.54	13.93	14.05	14.09
FeO	3.94	7.50	1.20	1.30	2.63	0.31
Fe_2O_3	2.09	8.12	0.93	–	1.41	–
Fe_2O_3T	6.47	16.45	2.26	2.47	4.33	0.77
MnO	0.08	0.24	0.04	0.03	0.05	0.02
MgO	2.97	5.87	0.50	0.65	1.10	0.05
CaO	2.56	9.30	2.01	1.12	2.67	0.84
Na_2O	3.60	1.17	3.22	2.80	2.94	4.04
K2O	3.00	0.89	4.07	5.96	3.53	3.97
P_2O_5	0.12	0.17	0.08	0.12	0.18	0.07
LOI	0.83	3.04	0.52	0.84	0.39	1.58
Total	**99.73**	**99.78**	**99.71**	**98.66**	**99.78**	**99.44**
Ag	0	0	0	-1	0	-1
As	1	2	1	3	1	9
Ba	487	80	726	650	1 044	520
Be	3	1	1	0	3	1
Bi	0	0	0	0	0	0
Cd	0	0	0	0	0	0
Ce	84	18	76	115	161	22
Cr	161	150	9	22	24	2
Cs	2	0	1	3	1	5
Cu	40	171	8	3	26	-1
Dy	4	6	3	4	5	1
Er	2	4	2	1	3	1
Eu	1	2	1	1	2	0
F	1 256	520	159	374	989	-50
Ga	21	23	16	18	20	21
Gd	6	6	4	7	8	2
Ge	2	2	1	1	1	1
Hf	5	3	5	5	8	1
Ho	1	1	1	1	1	0
La	42	7	47	59	82	14
Lu	0	0	0	0	0	0
Mo	4	1	4	0	3	0
Nb	11	7	4	15	14	4
Nd	33	15	30	53	63	8
Ni	67	99	12	9	16	4
Pb	30	25	64	48	26	47
Pr	9	3	8	14	18	2
Rb	158	32	89	215	111	143
Sb	0	8	0	-1	0	-1
Sc	14	30	5	5	8	2
Sm	6	4	6	10	11	2
Sn	3	3	2	1	3	1
Sr	208	147	176	180	212	165
Ta	1	0	0	1	1	0
Tb	1	1	0	1	1	0
Th	23	1	30	43	26	8
U	4	0	4	6	3	4
V	112	322	12	21	51	2
Y	25	38	16	20	28	9
Yb	2	3	1	1	2	1
Zn	98	145	26	41	57	10
Zr	183	112	181	170	231	35
La/Nb	4.0	1.1	11.3	3.9	6.0	3.1
Y/Nb	2.3	5.6	3.9	1.3	2.0	2.2
Ta/Yb	0.4	0.1	0.3	0.9	0.4	0.2
Zr/Nb	17.1	16.5	43.1	11.3	17.0	8.1

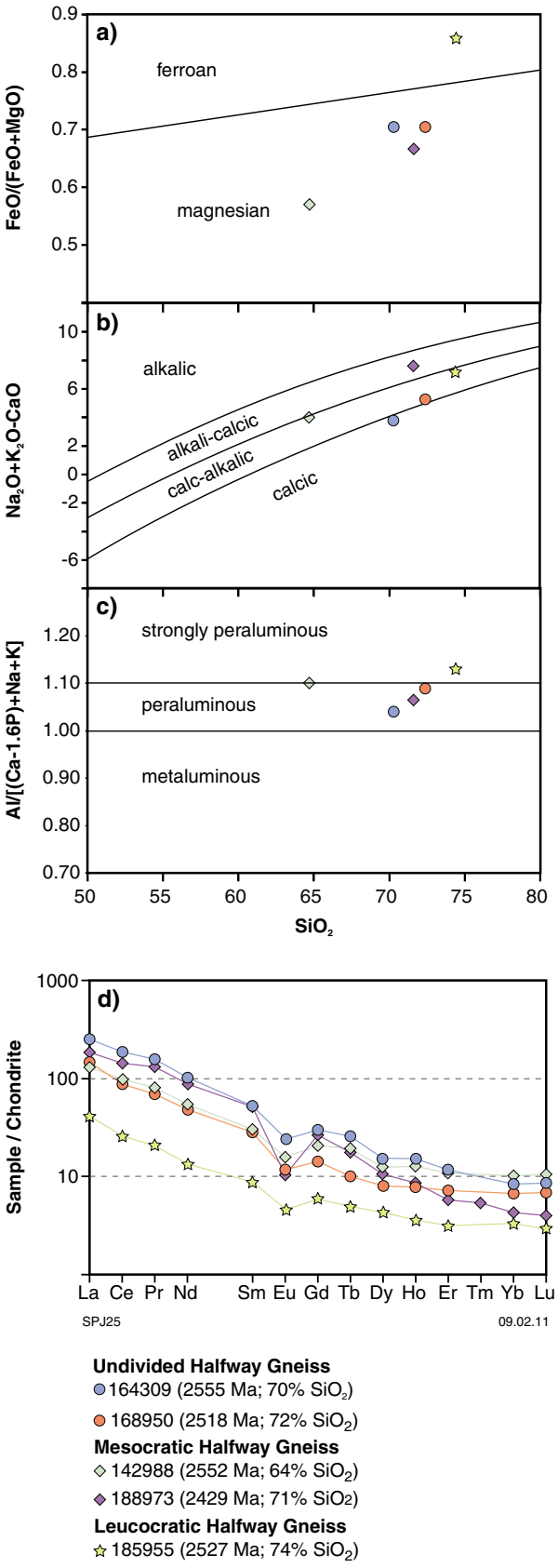

Figure 6. Whole-rock major, trace, and rare-earth element plots for Halfway Gneiss samples: a–c) compositional patterns of granitic gneisses of the Halfway Gneiss as a function of SiO_2 (wt%). Fields from Frost et al. (2001); d) chondrite-normalized (after Nakamura, 1974) REE plot of granitic gneisses of the Halfway Gneiss.

Undivided Halfway Gneiss

GSWA 164309: porphyritic biotite granodiorite gneiss, Middle Well

This sample was analysed by Nelson (2000b). The zircons are colourless to dark brown, mainly subhedral, strongly rounded, and equant to elongate. Although these zircons were not imaged under cathodoluminescence (CL), transmitted and reflected light images suggest that the grains are simple, without core or rims. Twenty-nine analyses are concordant to slightly discordant (Fig. 7a). One analysis >5% discordant is not considered further; the remaining 28 analyses can be divided into three groups. A coherent group of 18 analyses yields a concordia age of 2555 ± 4 Ma (MSWD = 1.7), interpreted as the crystallization age of the granodiorite protolith of the gneiss. This result is slightly older than the 2544 ± 5 Ma age proposed by Nelson (2000b). Eight analyses that yield $^{207}Pb^*/^{206}Pb^*$ dates of 2537–2501 Ma are interpreted to reflect ancient loss of radiogenic Pb. Two analyses yield $^{207}Pb^*/^{206}Pb^*$ dates of 2673 and 2605 Ma, interpreted as the ages of xenocrystic zircons. The age data are also shown in a probability density distribution plot (Fig. 8a).

GSWA 168950: pegmatite-banded tonalitic gneiss, Yandarra Well

This sample was analysed by Nelson (2001). The zircons isolated from this sample are pale yellow to dark brown, Mainly subhedral, strongly rounded, and equant to elongate. Although these zircons were not imaged under CL, transmitted and reflected light images suggest that the grains are simple, without differentiated core and rims. Twenty-eight analyses of 25 crystals are concordant to slightly discordant (Fig. 7b). Seven analyses >5% discordant or indicate high common Pb (f204 >1%) are not considered further. The remaining 21 analyses can be divided into three groups. Four analyses yield a weighted mean $^{207}Pb^*/^{206}Pb^*$ date of 2518 ± 2 Ma (MSWD = 0.22), interpreted as the crystallization age of the tonalitic protolith of the gneiss. Thirteen analyses yield $^{207}Pb^*/^{206}Pb^*$ dates of 2507–1919 Ma, interpreted to reflect ancient loss of radiogenic Pb. Four analyses yield $^{207}Pb^*/^{206}Pb^*$ dates of 2730–2619 Ma, interpreted as the ages of xenocrystic zircons. The age data are also shown in a probability density distribution plot (Fig. 8b).

NP21: granodiorite gneiss

Results for this sample were reported by Kinny et al. (2004). The zircons are mainly prismatic; several contain cores with concentric growth zoning surrounded by high-uranium, weakly zoned rims that are poorly luminescent in CL images. Fifteen analyses of 14 zircons are concordant to moderately discordant (Fig. 7c). Two analyses that are >5% discordant, and indicating about 5% common Pb (f204 >1%), are not considered further; of the remaining 13 analyses, six yield a weighted mean $207Pb^*/^{206}Pb^*$ date of 2508 ± 5 Ma (MSWD = 0.75), interpreted as the crystallization age of the gneiss' granodioritic protolith, and seven others yield $^{207}Pb^*/^{206}Pb^*$ dates of

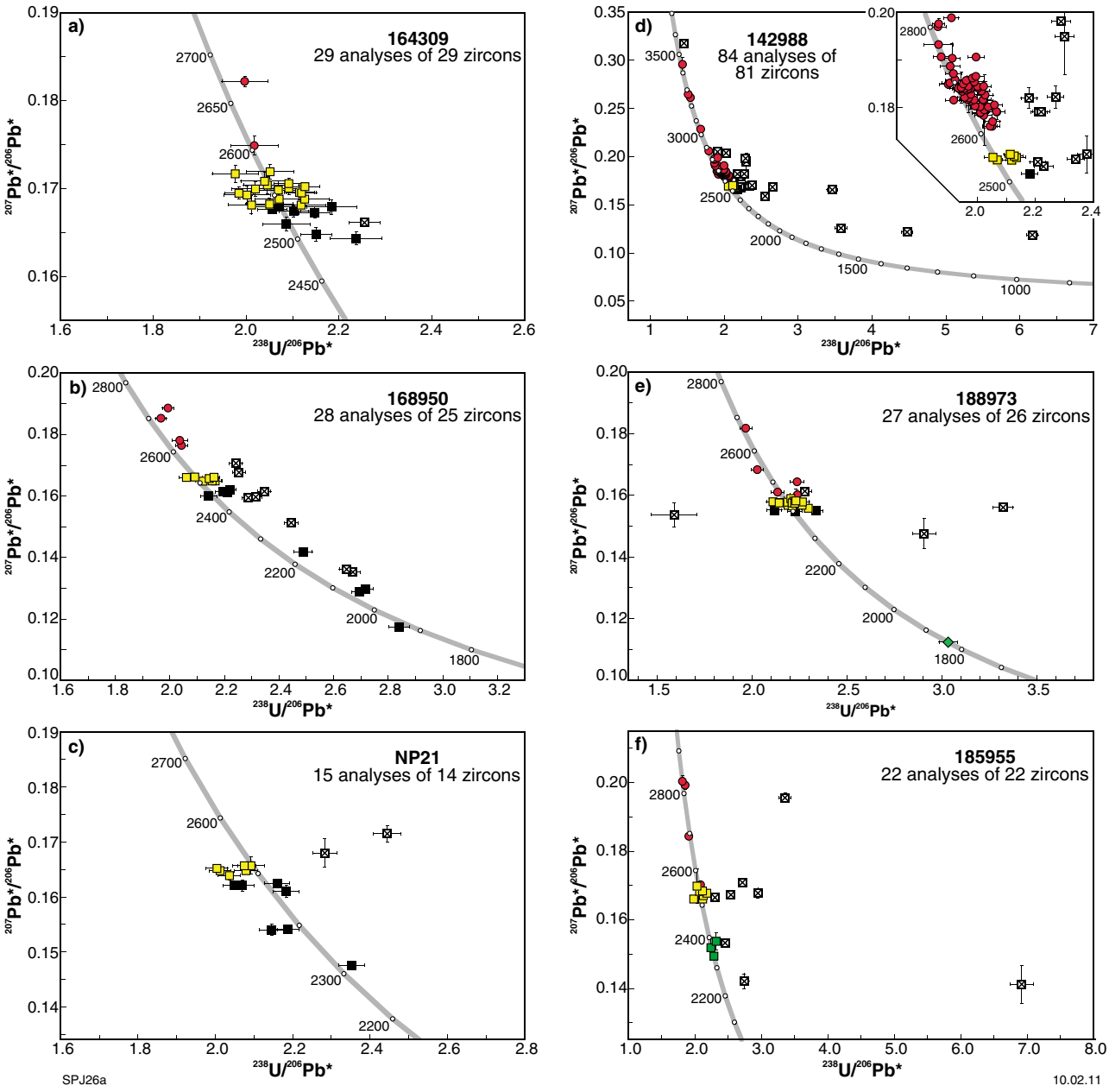

Figure 7. U–Pb analytical data for zircons from the Halfway Gneiss samples. Yellow squares indicate magmatic zircons, red circles indicate xenocrystic (inherited) zircons, green squares indicate zircons from later leucocratic veins, black squares indicate radiogenic-Pb loss, and crossed squares indicate data >5% discordant or indicating high common-Pb.

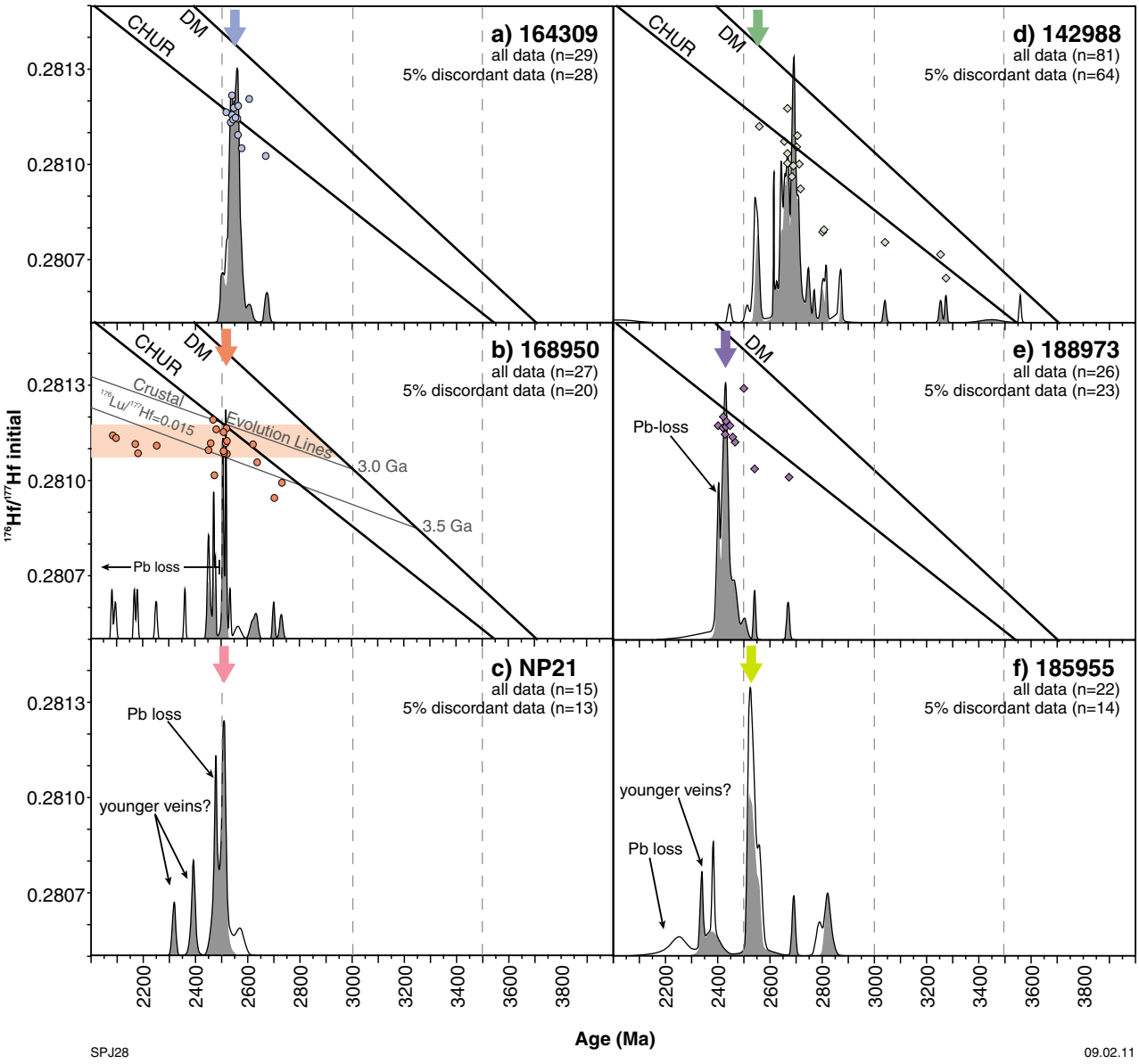

Figure 8. **Summary of age and Hf-isotope data for zircons from the Halfway Gneiss samples. The age data are plotted as probability density distributions; the grey shaded field includes data up to 5% discordant; the black curve includes all data. Coloured arrows above the density distributions show the timing of crystallization of the sample. Where Hf-isotope data are available, they are plotted as initial $^{176}Hf/^{177}Hf$ ratio verses $^{207}Pb/^{206}Pb$ age. Evolution lines for Depleted Mantle (DM) and Chondritic Uniform Reservoir (CHUR) are calculated using the values of Griffin et al. (2002). Crustal evolution lines (thin black lines) in part b) are calculated using an average continental crustal $^{176}Lu/^{177}Hf$ ratio of 0.015.**

2482–2318 Ma, interpreted to reflect ancient loss of radiogenic Pb. The age data are also shown in a probability density distribution plot (Fig. 8c). There is no obvious compositional difference between the three youngest analyses (2392–2318 Ma) and the older analyses, and therefore, contrary to the interpretation of Kinny et al. (2004), these young results are not interpreted as the ages of metamorphic zircons. However, they may date the crystallization of leucocratic veins within the gneiss. Zircon grains of similar age and origin have been dated within sample GSWA 185955.

Mesocratic Halfway Gneiss

GSWA 142988: biotite tonalite gneiss, Dunnawah Bore

Results for this sample were reported by Nelson (2000a), and additional data were obtained in 2005 (Wingate written comm., 2010). Zircons isolated from this sample are colourless to dark brown, anhedral to subhedral, and equant to elongate. CL imaging reveals that most crystals consist of zoned cores surrounded by structureless rims too thin to analyse successfully. Eighty-four analyses of 81 zircons are concordant to strongly discordant (Fig. 7d). Nineteen analyses >5% discordant are not considered further; the remaining analyses can be divided into three groups. Six analyses of six zircons yield a weighted mean $^{207}Pb^*/^{206}Pb^*$ date of 2552 ± 4 Ma (MSWD = 0.80), interpreted as the crystallization age of the tonalitic protolith of the gneiss. A single analysis, which yields a $^{207}Pb^*/^{206}Pb^*$ date of 2517 ± 4 Ma (1σ), is interpreted to reflect ancient loss of radiogenic Pb. Fifty-eight analyses of 58 zircons yield $^{207}Pb^*/^{206}Pb^*$ dates of 3447–2615 Ma, interpreted as the ages of xenocrystic zircons. Alternatively, the date of 2552 ± 4 Ma could represent the crystallization age of thin pegmatite veins within the rock; if this interpretation is correct, then the age of the tonalitic protolith would be c. 2615 Ma or older, but this interpretation is not preferred. The age data are also shown in a probability density distribution plot (Fig. 8d).

GSWA 188973: granodiorite gneiss, Pink Hills

This sample was analysed by Wingate et al. (written comm., 2010). The zircons are pale- to dark-brown, elongate, and subhedral to euhedral. Imaging under CL reveals that concentric growth zoning is ubiquitous, and texturally discordant cores are common. Twenty-seven analyses of 26 zircons are concordant to slightly discordant (Fig. 7e). Four analyses >5% discordant are not considered further; the remaining 23 analyses can be divided into four groups. Fourteen analyses yield a weighted mean $^{207}Pb^*/^{206}Pb^*$ date of 2429 ± 4 Ma (MSWD = 1.3), interpreted as the crystallization age of the granodiorite protolith. Three analyses, which yield $^{207}Pb^*/^{206}Pb^*$ dates of 2404–2400 Ma, are interpreted to reflect minor loss of radiogenic Pb. Five analyses yield $^{207}Pb^*/^{206}Pb^*$ dates of 2669–2457 Ma, interpreted as the ages of xenocrystic zircons. A single analysis of a zircon rim yields a $^{207}Pb^*/^{206}Pb^*$ date of 1838 ± 7 Ma (1σ), interpreted as the age of a metamorphic overprint. The age data are also shown in a probability density distribution plot (Fig. 8e).

Leucocratic Halfway Gneiss

GSWA 185955: leucocratic gneiss, Wabli Creek

This sample was analysed by Wingate et al. (2010). The sample yielded abundant zircons, which are colourless to dark brown, subhedral to euhedral, and equant to elongate. Many crystals are partially metamict. Most zircons have high uranium contents and show growth zoning; some also contain low-uranium zoned cores. Twenty-two analyses were obtained from 22 zircons, including one analysis of a high-uranium rim. The data are concordant to strongly discordant (Fig. 7f). Eight analyses, including the single rim analysis, are >5% discordant or indicate high common-Pb, and are not considered further. The remaining data can be divided into three groups. Seven analyses yield a weighted mean $^{207}Pb^*/^{206}Pb^*$ age of 2527 ± 9 Ma (MSWD = 1.7), interpreted as the crystallization age of the protolith to the gneiss. Four analyses indicate $^{207}Pb^*/^{206}Pb^*$ dates of 2829–2560 Ma, interpreted as the ages of inherited zircons, and three younger analyses yield a weighted mean $^{207}Pb^*/^{206}Pb^*$ age of 2342 ± 28 Ma (MSWD = 1.9), most likely date the crystallization of thin leucocratic veins within the gneiss. Zircon grains of similar age have been dated within sample NP21 (Kinny et al., 2004). The age data are also shown in a probability density distribution plot (Fig. 8f).

Zircon Lu–Hf isotope measurements

Magmatic and inherited zircons from four of the five dated samples were analysed by LA–ICP-MS to determine their Lu–Hf isotope ratios. These data are used to provide further information on the origins of the igneous precursors to the gneisses and the basement sources from which they originated, allowing inferences to be made about the tectonic setting of these units. Details of analytical procedures and Lu–Hf isotopic data are presented in Appendix 1. Initial $^{176}Hf/^{177}Hf$ ratios were calculated using the decay constant for ^{176}Lu (1.865×10^{-11}) proposed by Scherer et al. (2001), and the hafnium model ages ($T_{DM}^{crustal}$) were calculated from the observed initial hafnium isotopic ratio ($^{176}Lu/^{177}Hf$)t, and a $^{176}Lu/^{177}Hf$ ratio of 0.015 representing average continental crust (Griffin et al., 2002).

GSWA 164309: porphyritic biotite granodiorite gneiss, Middle Well

Fifteen zircons were selected for Lu–Hf analysis, of which 13 are interpreted to form a coherent group that dates the crystallization of the granodiorite protolith (2555 ± 4 Ma), although one of these has undergone minor Pb loss. The remaining two zircons are interpreted as xenocrysts.

The magmatic group indicates a narrow range of initial $^{176}Hf/^{177}Hf$ ratios of 0.281050–0.281216 (Fig. 8a; Table 3) that correspond to a range of εHf values between -3.1 and 1.9. The most radiogenic (i.e. the most juvenile) of these analyses lies between the Chondritic Uniform Reservoir (CHUR) and Depleted Mantle (DM) curves, and is similar in composition to a zircon xenocryst, dated at c. 2605 Ma, which has the most radiogenic composition with an initial $^{176}Hf/^{177}Hf$ ratio of 0.281205 (εHf = 3.1). It is possible that the main magmatic group were derived either from a juvenile mantle-derived source or from the recycling of older juvenile crustal material with a composition similar to that of the c. 2605 Ma zircon xenocryst. The other zircon xenocryst dated at c. 2675 Ma has a composition that is less radiogenic than CHUR, with a $^{176}Hf/^{177}Hf$ ratio and εHf value of 0.281015 and -2.1, respectively.

GSWA 168950: pegmatite-banded tonalitic gneiss, Yandarra Well

Twenty-three zircons yielding U–Pb results <5% discordant were selected for Lu–Hf analysis. Six crystals yielded a date of 2518 ± 2 Ma, interpreted as the crystallization age of the tonalite protolith. Four zircons are interpreted as xenocrysts, and the remaining 13 zircons are interpreted to have lost radiogenic Pb (but not enough to render them >5% discordant) during a metamorphic event at c. 1855 Ma. These latter crystals were analysed to assess the effects of Pb-loss and the coupling of the U–Pb and Lu–Hf systems during metamorphism. The six magmatic crystals yield initial $^{176}Hf/^{177}Hf$ compositions that are nonradiogenic with respect to CHUR (0.281084–0.281163; Fig. 8b; Table 3), corresponding to εHf values between -3.5 and -0.4 (Table 3). The four xenocrysts, dated between 2730 and 2620 Ma, have a range of initial $^{176}Hf/^{177}Hf$ ratios (0.280945–0.281113) and εHf values (-4.0 to 0.4) that are equal to, or less radiogenic than, CHUR (Fig. 8b; Table 3). The remaining 13 zircons that have undergone variable amounts of Pb-loss yield similar compositions to the six magmatic crystals. Their initial $^{176}Hf/^{177}Hf$ compositions are between 0.281016 and 0.281190, with εHf values between -13.1 and -0.4 (Table 3). This narrow range of initial $^{176}Hf/^{177}Hf$ compositions supports a model in which the magmatic zircons lost minor amounts of radiogenic lead, presumably during the c. 1855 Ma metamorphic event, but did not lose any radiogenic hafnium.

GSWA 142988: biotite tonalite gneiss, Dunnawah Bore

Of the 16 zircons selected for Lu–Hf analysis, one is from the group interpreted to date crystallization of the tonalite protolith at 2552 ± 4 Ma, and the remaining 15 are xenocrystic zircons. The single magmatic crystal (2558 Ma) indicates an initial $^{176}Hf/^{177}Hf$ composition of 0.281119 and a εHf value of -1.1. The 15 xenocrysts, dated between 3274 and 2655 Ma, yield a wide range of initial $^{176}Hf/^{177}Hf$ compositions (0.280788–0.281090), and corresponding εHf values of -7.2 to 3.4 (Table 3; Fig. 8d), plotting below and above the CHUR reference line.

GSWA 188973: granodiorite gneiss, Pink Hills

Twelve zircons were selected for Lu–Hf analyses. Nine of these zircons are from the group that dates crystallization of the granodiorite protolith at 2429 ± 4 Ma, and three zircons are interpreted to be xenocrysts. The nine magmatic crystals have a very narrow range of initial $^{176}Hf/^{177}Hf$ compositions (0.281123–0.281205; εHf = -3.0 to -1.2; Table 3; Fig. 8e) that are slightly less radiogenic than CHUR. The youngest inherited zircon, dated at c. 2500 Ma, has the most radiogenic composition, with an initial $^{176}Hf/^{177}Hf$ of 0.281293 and an εHf value of 3.8. The two older inherited zircons, dated at c. 2540 and c. 2670 Ma, have less radiogenic compositions, with initial $^{176}Hf/^{177}Hf$ of 0.281041 and 0.281025, and εHf values of -4.3 and -1.9, respectively.

Discussion

Tectono-magmatic evolution

Age components of the Halfway Gneiss

Protoliths of the six dated Halfway Gneiss samples have a range of crystallization ages between 2555 and 2429 Ma. Each sample contains inherited zircons that provide information on the basement from which these rocks were sourced, or with which these rocks interacted during emplacement. The majority of these zircons yield ages that are similar to the crystallization ages of the gneiss protoliths. In total, 51% (72 of 141 analyses) of all analysed zircons (both magmatic and inherited) are the same age as, or younger than, the oldest dated gneiss protolith at c. 2555 Ma. Thirty-seven percent (53 of 141 analyses) have ages between 2730 and 2600 Ma, whereas 16 analyses or 12% have older ages between 3447 to 2730 Ma (Figs 7–9). The group of analyses with ages between 2730 and 2600 Ma are predominantly from a single sample (GSWA 142988), and one possible interpretation is that they date the crystallization age of the gneiss, with the younger age population at 2552 ± 4 Ma dating the age of leucocratic veins within the gneiss. Irrespective of this interpretation, similar aged (2715–2600 Ma) inherited zircons are present within most of the other samples (GSWA 185955, 188973, 168950, and 164309), indicating that crust of this age either forms a large component of the Halfway Gneiss, or played a major role in the genesis of the gneiss protoliths. The oldest population of zircons indicates that some Paleo- to Mesoarchean crust is present within, or was involved in the formation of, the Halfway Gneiss. Two samples (NP21 and GSWA 185955) yield rare magmatic grains with ages between 2392–2318 Ma. These are interpreted to date the crystallization of thin leucocratic veins within the samples.

Isotopic evolution

Collectively, most magmatic and inherited zircons analysed yield a narrow range of initial $^{176}Hf/^{177}Hf$ compositions that are similar to, or slightly less radiogenic than, CHUR

Table 3. Summary of zircon Hf-isotope data

Geochron ID	*Analysis no.*	*$^{207}Pb/^{206}Pb$ date (Ma)*	*$^{176}Hf/^{177}Hf$ measured*	*1σ*	*$^{176}Lu/^{177}Hf$ measured*	*$^{176}Yb/^{177}Hf$ measured*	*$^{176}Hf/^{177}Hf$ initial*	*epsilon Hf*	*1 std error*	*$T_{(DM)}$ crustal (Ga)*	*Zircon type*	*Group*
Undivided Halfway Gneiss												
164309	1.1	2560	0.281246	0.000026	0.002086	0.058487	0.281144	-0.2	0.9	3.1	magmatic	G
	2.1	2563	0.281243	0.000034	0.001233	0.033703	0.281183	1.3	1.2	3.0	magmatic	G
	3.1	2534	0.281185	0.000028	0.001103	0.037499	0.281132	-1.2	1.0	3.1	magmatic	G
	5.1	2553	0.281180	0.000013	0.000687	0.023413	0.281146	-0.2	0.5	3.1	magmatic	G
	6.1	2553	0.281179	0.000022	0.000867	0.031802	0.281137	-0.6	0.8	3.1	magmatic	G
	13.1	2566	0.281194	0.000019	0.001107	0.039080	0.281140	-0.2	0.7	3.1	magmatic	G
	15.1	2517	0.281197	0.000016	0.000704	0.024175	0.281163	-0.5	0.6	3.1	Pb loss	-
	17.1	2537	0.281186	0.000013	0.000628	0.021058	0.281156	-0.3	0.5	3.1	magmatic	G
	19.1	2605	0.281236	0.000016	0.000622	0.019315	0.281205	3.1	0.6	2.9	inherited	F
	21.1	2562	0.281134	0.000018	0.000862	0.027096	0.281092	-2.0	0.6	3.2	magmatic	G
	24.1	2546	0.281220	0.000012	0.000896	0.028355	0.281176	0.7	0.4	3.0	magmatic	G
	25.1	2673	0.281027	0.000022	0.000232	0.007264	0.281015	-2.1	0.8	3.3	inherited	E
	26.1	2576	0.281088	0.000015	0.000766	0.024275	0.281050	-3.1	0.5	3.3	magmatic	G
	28.1	2546	0.281205	0.000017	0.001333	0.038111	0.281140	-0.6	0.6	3.1	magmatic	G
	29.1	2539	0.281248	0.000018	0.000662	0.019819	0.281216	1.9	0.6	2.9	magmatic	G
168950	1.1	2506	0.281121	0.000006	0.000625	0.032041	0.281091	-3.3	0.2	3.2	Pb loss	-
	2.1	2471	0.281100	0.000008	0.001780	0.088567	0.281016	-6.8	0.3	3.4	Pb loss	-
	3.1	2518	0.281152	0.000009	0.000601	0.036244	0.281123	-1.9	0.3	3.2	magmatic	H
	4.1	2251	0.281141	0.000013	0.000714	0.031797	0.281110	-8.5	0.5	3.4	Pb loss	-
	5.1	2456	0.281127	0.000012	0.000227	0.013264	0.281116	-3.5	0.4	3.2	Pb loss	-
	6.1	2635	0.281092	0.000011	0.000702	0.036276	0.281057	-1.5	0.4	3.2	inherited	F
	7.1	1919	0.281245	0.000011	0.001406	0.042090	0.281194	-13.1	0.4	3.4	Pb loss	-
	8.1	2519	0.281105	0.000007	0.000479	0.020540	0.281082	-3.3	0.3	3.3	magmatic	H
	9.1	2507	0.281117	0.000013	0.000690	0.041587	0.281084	-3.5	0.5	3.3	magmatic	H
	10.1	2564	0.281152	0.000447	0.025597	0.281130	0.000010	-0.6	0.3	3.1	inherited	G
	11.1	2478	0.281187	0.000011	0.000560	0.032601	0.281161	-1.5	0.4	3.1	Pb loss	-
	12.1	2449	0.281109	0.000012	0.000303	0.018000	0.281095	-4.5	0.4	3.3	Pb loss	-
	13.1	2701	0.281010	0.000014	0.001260	0.067265	0.280945	-4.0	0.5	3.4	inherited	D
	14.1	2730	0.281073	0.000012	0.001540	0.081686	0.280993	-1.6	0.4	3.3	inherited	D
	15.1	2619	0.281154	0.000013	0.000823	0.040745	0.281113	0.1	0.5	3.1	inherited	F
	15.2	2534	0.281900	0.000013	0.000565	0.031019	0.281163	-0.4	0.5	3.1	magmatic	G
	16.1	2519	0.281132	0.000842	0.043136	0.281092	0.000011	-3.0	0.4	3.2	inherited	H
	17.1	2466	0.281194	0.000012	0.000075	0.004954	0.281190	-0.7	0.4	3.0	Pb loss	-
	17.2	2082	0.281164	0.000010	0.000527	0.029126	0.281143	-11.2	0.3	3.4	Pb loss	-
	18.1	2095	0.281157	0.000010	0.000554	0.029599	0.281135	-11.2	0.4	3.4	Pb loss	-
	19.1	2179	0.281104	0.000012	0.000429	0.028713	0.281086	-11.0	0.4	3.5	Pb loss	-
	20.1	2168	0.281127	0.000008	0.000274	0.016915	0.281116	-10.2	0.3	3.4	Pb loss	-
	20.2	2506	0.281160	0.000012	0.000197	0.010743	0.281151	-1.2	0.4	3.1	Pb loss	-
	21.1	2472	0.281134	0.000708	0.042113	0.281101	0.000009	-3.7	0.3	3.2	magmatic	I
	22.1	2507	0.281119	0.000009	0.000565	0.033149	0.281092	-3.2	0.3	3.2	magmatic	H
	23.1	2515	0.281126	0.000011	0.000189	0.010377	0.281117	-2.2	0.4	3.2	magmatic	H

Table 3. (continued)

Geochron ID	Analysis no.	$^{207}Pb/^{206}Pb$ date (Ma)	$^{176}Hf/^{177}Hf$ measured	1σ	$^{176}Lu/^{177}Hf$ measured	$^{176}Yb/^{177}Hf$ measured	$^{176}Hf/^{177}Hf$ initial	epsilon Hf	1 std error	$T_{(DM)}$ crustal (Ga)	Zircon type	Group
Mesocratic Halfway Gneiss												
142988	1.1	2806	0.280852	0.000015	0.001060	0.047229	0.280795	-6.9	0.5	3.7	inherited	C
	3.1	2558	0.281176	0.000014	0.001172	0.045702	0.281119	-1.1	0.5	3.1	magmatic	G
	5.1	2701	0.281122	0.000011	0.001286	0.056760	0.281056	0.0	0.4	3.2	inherited	D
	6.1	3253	0.280774	0.000013	0.000902	0.037836	0.280718	0.8	0.5	3.6	inherited	A
	7.1	2666	0.281206	0.000010	0.000618	0.022574	0.281174	3.4	0.4	2.9	inherited	E
	8.1	2667	0.281101	0.000014	0.001318	0.056934	0.281034	-1.6	0.5	3.3	inherited	E
	9.1	2704	0.281142	0.000010	0.001009	0.042690	0.281090	1.2	0.4	3.1	inherited	D
	15.1	2655	0.281108	0.000008	0.000716	0.030861	0.281072	-0.5	0.3	3.2	inherited	E
	16.1	2711	0.281081	0.000011	0.001551	0.065746	0.281001	-1.8	0.4	3.3	inherited	D
	17.1	2801	0.280827	0.000009	0.000729	0.030728	0.280788	-7.2	0.3	3.7	inherited	C
	20.1	3040	0.280808	0.000009	0.000899	0.036580	0.280756	-2.8	0.3	3.6	inherited	B
	21.1	2689	0.281033	0.000010	0.000743	0.031856	0.280995	-2.5	0.4	3.3	inherited	E
	23.1	2683	0.280999	0.000007	0.000734	0.031839	0.280961	-3.8	0.2	3.4	inherited	E
	24.1	3274	0.280701	0.000007	0.000915	0.036772	0.280643	-1.4	0.2	3.7	inherited	A
	26.1	2667	0.281068	0.000013	0.001270	0.060972	0.281003	-2.7	0.5	3.3	inherited	E
	28.1	2716	0.280964	0.000011	0.000795	0.037581	0.280923	-4.4	0.4	3.5	inherited	
188973	2.1	2419	0.281214	0.000013	0.000976	0.047891	0.281169	-2.5	0.5	3.1	magmatic	J
	7.1	2457	0.281196	0.000012	0.001177	0.043967	0.281141	-2.6	0.4	3.2	magmatic	I
	8.1	2669	0.281082	0.000016	0.001117	0.050152	0.281025	-1.9	0.6	3.3	inherited	E
	10.1	2421	0.281234	0.000011	0.000633	0.029098	0.281205	-1.2	0.4	3.0	magmatic	J
	11.1	2387	0.281240	0.000782	0.035950	0.281204	0.000013	-2.0	0.5	3.1	magmatic	J
	12.1	2466	0.281167	0.000015	0.000926	0.041717	0.281123	-3.1	0.5	3.2	magmatic	I
	13.1	2432	0.281229	0.000010	0.000843	0.036155	0.281190	-1.5	0.4	3.1	magmatic	J
	14.1	2401	0.281241	0.000011	0.001417	0.060308	0.281176	-2.7	0.4	3.1	magmatic	J
	15.1	2541	0.281082	0.000009	0.000846	0.033418	0.281041	-4.3	0.3	3.3	inherited	G
	16.1	2445	0.281229	0.000007	0.001115	0.048109	0.281177	-1.6	0.2	3.1	magmatic	I
	17.1	2501	0.281336	0.000007	0.000898	0.035960	0.281293	3.8	0.3	2.8	inherited	H
	22.1	2429	0.281202	0.000011	0.000630	0.028830	0.281173	-2.1	0.4	3.1	magmatic	J
	24.1	2428	0.281205	0.000013	0.001207	0.054466	0.281149	-3.0	0.5	3.2	magmatic	J

(Figs 8 and 9). This implies that most zircons crystallized from melts with a 'mixed' source, involving variable proportions of both juvenile mantle-derived material (DM-source), and an older crustal component. This is reflected by the older $T_{DM}^{crustal}$ Hf model ages for the zircons (3700 to 2900 Ma) compared to their U–Pb crystallization ages, which range from 3447 to 2429 Ma (Fig. 9).

The isotopic evolution of the Halfway Gneiss and its inherited components are best represented on an 'event signature' plot (Fig. 10a), in which the hafnium isotopic data are simplified by averaging the model ages for each of the main age peaks, thus reducing the data to an 'event signature' curve that shows the main features of crustal evolution (Griffin et al., 2006; Belousova et al., 2009). The simplified model age and age peak data are presented in Table 4. On the event signature plot, reworking of older crust produces a downward trend with decreasing age, whereas juvenile inputs (leading to a lower mean crustal residence source age) produce rising trends with decreasing age. Trends of intermediate slope imply contributions from both juvenile and pre-existing crust.

Table 4. Mean age and average mean crustal residence age (MCRA) of analysed zircon

Group	*Age (Ma)*	*MCRA average*
A	3264	-367
B	3040	-582
C	2804	-905
D	2711	-590
E	2671	-580
F	2620	-464
G	2552	-556
H	2512	-644
I	2460	-712
J	2417	-682

>3500 to 2800 Ma

The presence of a limited number of inherited zircons (ten), ranging in age from 3447 to 2801 Ma, suggests a Paleo- to Mesoarchean history for the Halfway Gneiss (Fig. 10a), which was recycled over this period without any juvenile additions. However, the eight oldest zircons are from a single sample (GSWA 142988, dated at c. 2555 Ma), and thus it is not clear whether they indicate the presence of an old, widespread, basement to the Halfway Gneiss, or whether they reflect limited interaction with an older, possibly sedimentary, component. Irrespective of this, the younger zircons analysed in this study (2730–2430 Ma) have similar hafnium crustal model ages (3500–3000 Ma) to the crystallization ages of the inherited zircons (3450–2800 Ma). Also, the five oldest inherited zircons analysed for hafnium isotopes have similar hafnium crustal

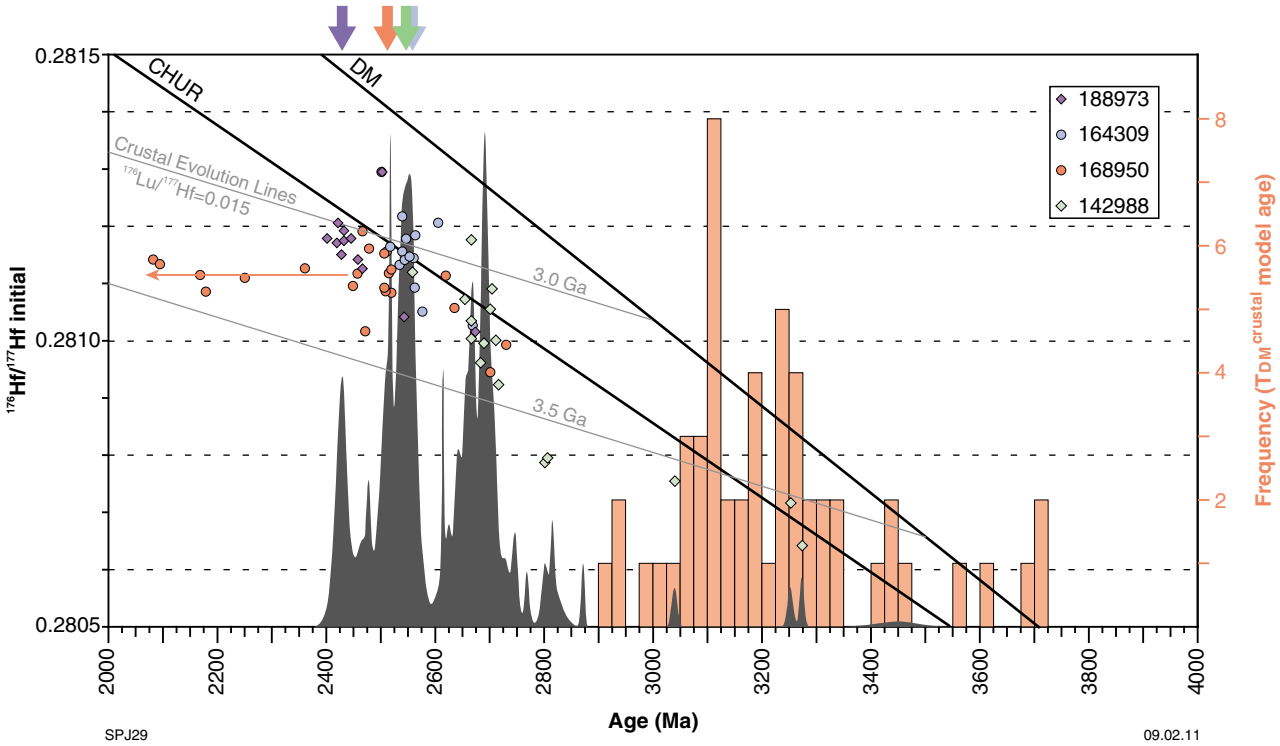

Figure 9. Compilation of age and Lu–Hf isotope data for zircons from the Halfway Gneiss. Coloured dots and diamonds show the initial $^{176}Hf/^{177}Hf$ ratios of the zircons. Evolution lines for 3.0 Ga and 3.5 Ga crust are shown for reference. The corresponding hafnium crustal model ages ($T_{DM}^{crustal}$) for the zircons are plotted as orange bars in the histogram. Model ages are calculated using an average continental crustal $^{176}Lu/^{177}Hf$ ratio of 0.015. The probability density distribution (grey shaded field) displays the $^{207}Pb^*/^{206}Pb^*$ dates for inherited and magmatic zircons that are <5% discordant (n=141). The coloured arrows show the interpreted crystallization age for each gneiss sample.

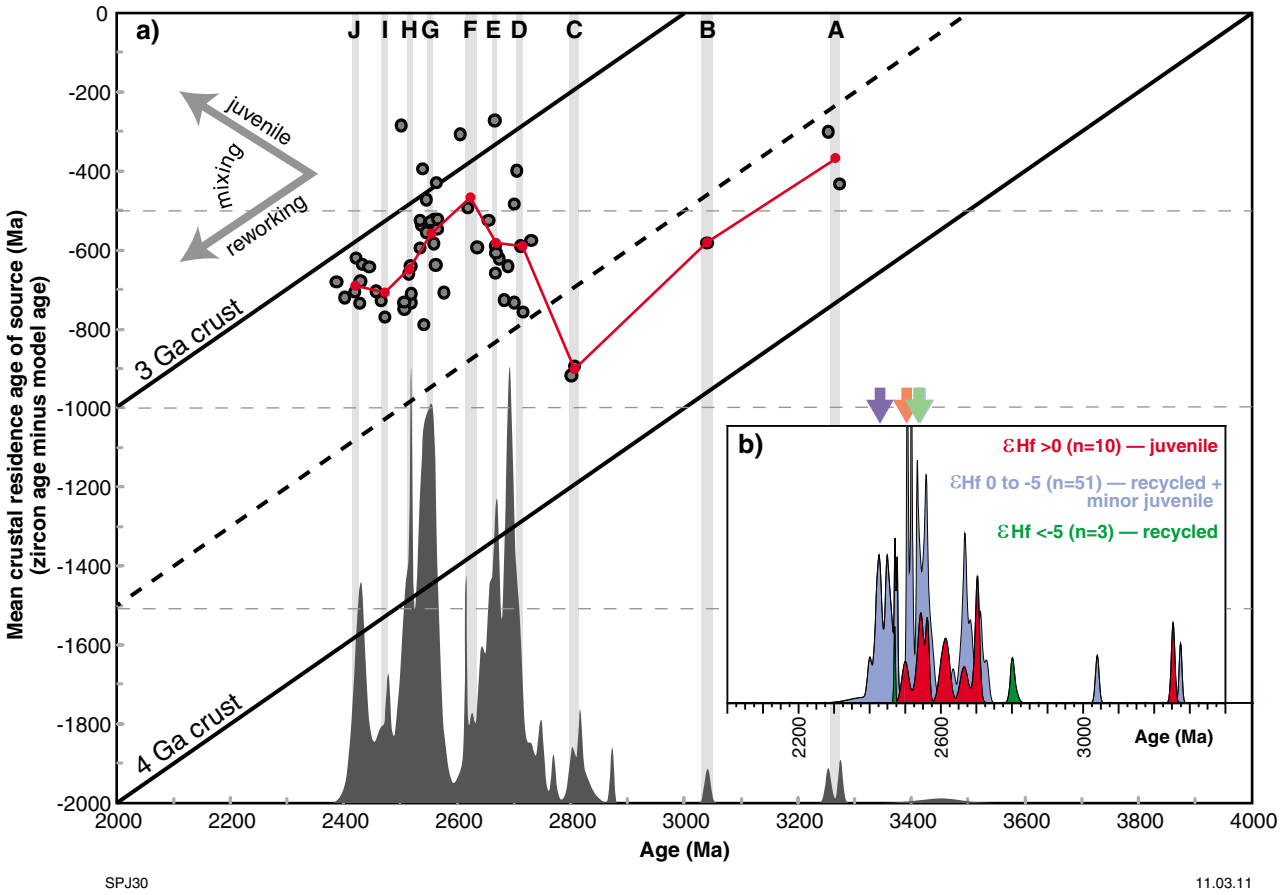

Figure 10. a) event signature plot of Hf-isotope data for zircons from Halfway Gneiss samples, where the mean magma source residence time (zircon age minus $T_{DM}^{crustal}$) is plotted against age. Inherited and magmatic zircon analyses from the Halfway Gneiss that are <5% discordant are shown as a probability density distribution (n=141; dark grey area). Light grey vertical lines show the ages for which the Hf-isotope data are averaged, the data summarized in Table 4; b) probability density diagram showing the relative abundance of zircons with εHf >0 (juvenile source), εHf 0 to -5 (mixed source), and εHf <-5 (recycled source). The coloured arrows show the interpreted crystallization age for each gneiss sample.

model ages (3700–3500 Ma). These isotopic data imply derivation of all gneiss protoliths from an isotopically uniform crustal source; i.e. an older, widespread, isotopically juvenile basement that was extracted from the depleted mantle sometime between 3700 and 3500 Ma. However, without additional age and isotopic data from the Halfway Gneiss, it is not possible to speculate further on the presence or nature of this older crust.

2730 to 2600 Ma

The large number of inherited magmatic grains dated between 2730 and 2600 Ma records a period of significant crustal growth. These magmatic zircons have hafnium isotopic ratios that are mostly more radiogenic than CHUR (εHf up to 3.4; Figs 8–10). Combined with the significant upward trend displayed on the event signature plot (Fig. 10a), these data indicate that crustal growth occurred predominantly via the input of juvenile magmatic components. However, the presence of some zircons with less radiogenic compositions (Fig. 9; εHf down to -2.7) suggests that there was limited mixing with, or assimilation of, an older crustal component (either in the form of basement to the gneisses or as a sedimentary component). This is reflected by the older crustal model ages for all of the <2730 Ma zircons (3500–3000 Ma), and the presence of limited zircon xenocrysts with crystallization ages (3450–2730 Ma) similar to the crustal model ages.

These data imply a geological setting in which large volumes of granitic material were generated from a juvenile source, and which were added to, and partially assimilated or mixed with, older Paleo- to Mesoarchean crust. The most common tectonic setting for such a scenario on the modern Earth is a suprasubduction zone, especially that of a continental-margin arc. Another possibility is the emplacement of a mantle plume derived large igneous province into older continental crust; however, the distinct lack of mafic material within the Halfway Gneiss suggests that this latter scenario is unlikely.

2600 to 2430 Ma

Much of the Halfway Gneiss (i.e. 51% of all dated zircons and all of the dated rocks) crystallized between 2600 and 2430 Ma, representing a significant episode of magmatism

in the Glenburgh Terrane. In the event signature plot (Fig. 10a), the dated magmatic and inherited zircons between 2600 and 2430 Ma (including the c. 2555 Ma population within GSWA 142988) reveal a downward trend characteristic of the reworking of older crust. The majority of these zircons have hafnium crustal model ages ($T_{DM}^{crustal}$ = 3500–3000 Ma; Table 3) that are indistinguishable from those of rocks formed during the 2730–2600 Ma event (Fig. 10a), suggesting that the 2600–2430 Ma rocks were derived by major crustal-scale reworking of pre-existing 2730–2600 Ma crust. This is compatible with the presence of abundant 2730–2600 Ma inherited zircons in the dated samples. However, one sample (GSWA 164309) contains magmatic zircons (dated at 2555 Ma) with a range of isotopic compositions (Fig. 8a), including four that are more radiogenic than CHUR (εHf = 0.7 to 3.1). A similar aged (c. 2500 Ma; Figs 7e and 8e) and similarly radiogenic (εHf = 3.8; Fig. 7e) zircon xenocryst is present in GSWA 188973. The juvenile composition of these grains may suggest that some juvenile mantle-derived material was involved in the formation of these gneisses (Fig. 10b). Alternatively, the juvenile compositions may have been inherited from the recycling of limited, but equally juvenile, crust formed during the 2730–2600 Ma magmatic episode; i.e. those that plot above the 3 Ga crust reference line in Figure 10a.

All the 2600–2430 Ma gneisses (including GSWA 142988, if its crystallization age is c. 2555 Ma) have 'mixed' isotopic signatures, and share similar major, trace, and REE compositions to each other (Fig. 6a–d). The hafnium isotopic information indicates that these granitic rocks were derived predominantly from the reworking of older crust with only very limited input of new juvenile material. The chemistry of these granites is therefore more likely to reflect that of the recycled components rather than of the source materials. Thus, the relatively shallowly sloping chondrite-normalized REE patterns (Fig. 6d) and low concentrations of the trace elements La, Nb, Y, Ta, and Yb, which are usually considered characteristic of suprasubduction zone granitic magmas (Pearce et al., 1984), are more likely to have been inherited from the pre-existing 2730–2600 Ma crust, and do not reflect the tectonic setting of the 2600–2430 Ma rocks.

Summary

The presence of inherited zircons with ages older than 2800 Ma, in combination with old hafnium crustal model ages (3700–3500 Ma) of all zircons from the Halfway Gneiss, hint at the presence of a Paleo- to Mesoarchean crustal component in the Glenburgh Terrane.

From 2730–2600 Ma, inherited zircons record the input of significant juvenile material. However, the magmatic zircons in this age range have much older crustal model ages, implying the presence of an older unradiogenic source, such as crust or sediments, with which these magmas interacted. It is possible that the 2730–2600 Ma material formed by suprasubduction processes in a continental-margin arc. The majority of the Halfway Gneiss formed between 2600 and 2430 Ma, mainly through the reworking of older gneisses.

Is the Glenburgh Terrane exotic to the Yilgarn and Pilbara Cratons?

Present models for the amalgamation of the West Australian Craton interpret the Glenburgh Terrane as exotic to both the Pilbara and Yilgarn Cratons (Martin and Morris, 2010; Johnson et al., 2010b). This hypothesis is supported by the MT survey (Selway, 2008; Selway et al., 2009), which shows that the Glenburgh Terrane has a distinctly different electrical character from that of the bounding cratons (Fig. 3); i.e. it is more conductive than the highly resistive cratons. However, it is possible that this conductive crust could have been produced by the wholescale reworking and addition of 2555–2430 Ma material into the margin of either the Pilbara or Yilgarn Cratons. In light of abundant geochronological and isotopic information available for the magmatic and volcanosedimentary material that makes up these cratons, a more robust comparison can be made with the Halfway Gneiss in order to test these alternate models.

Pilbara Craton

The boundary between the Glenburgh Terrane and Pilbara Craton is not exposed, being covered by extensive sedimentary deposits of the Paleoproterozoic Ashburton Basin, and the Mesoproterozoic Edmund and Collier Basins. The MT survey (Selway, 2008; Selway et al., 2009) showed that there is a major change in resistivity across a steeply dipping structure, roughly coinciding at the surface with the Talga Fault (Fig. 3). Although the Glenburgh Terrane is not exposed in the northern part of the Gascoyne Province, the region of high conductivity is interpreted to represent crust, exotic to the Pilbara Craton, where it forms basement to voluminous younger magmatic rocks that were extensively deformed and reworked during the Paleo- to Neoproterozoic (Sheppard et al., 2010b). Alternatively, the southern Pilbara Craton could have been the site of multiple magmatic and reworking events, rendering it highly conductive.

During the Archean, the Pilbara Craton was dominated by the construction of granite–greenstone terranes prior to 2800 Ma (e.g. Van Kranendonk et al., 2007). These rocks are unconformably overlain by the late Archean to Paleoproterozoic volcanic and sedimentary rocks of the Hamersley, Fortescue, and Turee Creek Groups (Fig. 11). These rocks are in turn unconformably overlain by volcanic and sedimentary rocks of the c. 2200 Ma lower Ashburton Basin (Thorne and Seymour, 1991), specifically the lower Wyloo Group (Fig. 11). The geochronological, geochemical, and isotopic evolution of these 3700–2830 Ma granite–greenstone terranes is well constrained (e.g. Van Kranendonk et al., 2007). In addition, key volcanic and volcaniclastic horizons within the overlying volcanosedimentary groups (Fig. 11) have been precisely dated (Barley et al., 1997; Trendall et al., 1998; Pickard, 2002; Rasmussen et al., 2005a), allowing the construction of a well-defined, basin-scale stratigraphy (e.g. Trendall et al., 2004). However, little information exists on the isotopic composition, or geochemical evolution, of these volcanic and volcaniclastic rocks. Even fewer age and isotopic data exist for the overlying lower Wyloo Group.

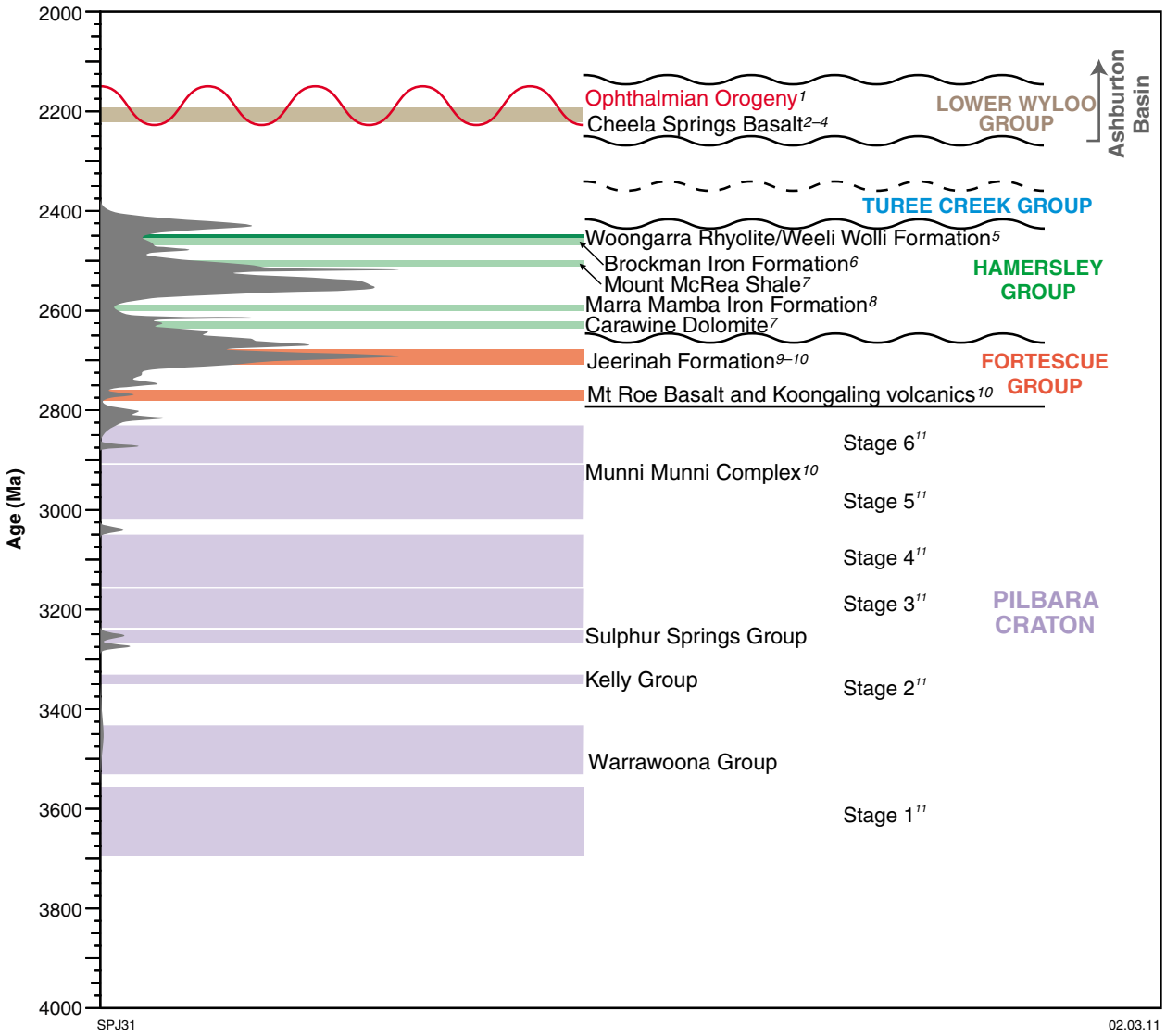

Figure 11. Summary of geological events in the Pilbara Craton, and depositional ages of metasedimentary packages from the Hamersley, Fortescue and Turee Creek Groups, and Ashburton Basin along the southern margin of the Pilbara Craton. Overlain in dark grey is a probability density curve of zircon ages for Halfway Gneiss samples as in Figures 9 and 10 (n=141). Red wavy line indicates the age of the Ophthalmian Orogeny. Superscripts indicate age references: 1 — Rasmussen et al. (2005b); 2 — Müller et al. (2005); 3 — Martin et al. (1998); 4 — Martin et al. (1998); 5 — Barley et al. (1997); 6 — Pickard (2002); 7 — Rasmussen et al. (2005a); 8 — Trendall et al. (1998); 9 — Rasmussen and Fletcher (2010); 10 — Arndt et al. (1991); 11 — Van Kranendonk et al. (2007).

Correlation between the Halfway Gneiss and southern Pilbara Craton can be tested by comparing their magmatic histories. The currently available geochronological information is summarized in Figure 11. Although the bulk of the Halfway Gneiss is younger than c. 2555 Ma, the presence of older (greater than 2600 Ma) inherited zircons, and old hafnium crustal model ages (3700–3000 Ma) of magmatic zircons, indicate the presence of an older crustal component up to 3700 Ma. This is broadly compatible with age data from the Pilbara granite–greenstone terranes (Fig. 11). However, the number of inherited zircons older than c. 2800 Ma is far too small to permit meaningful comparison.

The timing of peak magmatism and crustal growth within the Halfway Gneiss broadly coincides with the ages of volcanism and sedimentation in the Fortescue, Hamersley, and Turee Creek Groups between 2800 and 2430 Ma (Fig. 11), but there is little correspondence between the ages of individual volcanic or magmatic units within the basin and those within the Halfway Gneiss (Fig. 11). This argues against a connection between the Glenburgh Terrane and Pilbara Craton until at least the time of the Ophthalmian Orogeny (2215–2145 Ma; Fig. 11), an event which may have been responsible for deposition of the sedimentary precursors to the Moogie Metamorphics across much of the Glenburgh Terrane (Johnson et al., 2010b). The geochronological and MT data are consistent with the juxtaposition of an old, cold, and electrically resistive Pilbara Craton with a young, hot, exotic block (Halfway Gneiss) along a suture coincident with the present-day Talga Fault.

Yilgarn Craton

The boundary between the Glenburgh Terrane and Yilgarn Craton is marked by the Errabiddy Shear Zone (Figs 1, 2, and 4), which is shown in the MT survey (Selway, 2008; Selway et al., 2009) to be a moderately south-dipping structure (Fig. 3). This zone is up to 25 km wide and separates the highly conductive crust of the Glenburgh Terrane from the more resistive crust of the Yilgarn Craton (Fig. 3). At the surface, the zone contains imbricate slices of strongly deformed metagranitic rocks and gneisses of the Yilgarn Craton, and high-grade metasedimentary rocks of the Glenburgh Terrane (Camel Hills Metamorphics; Fig. 2). SHRIMP dating of metamorphic zircon and monazite from the high-grade metasedimentary rocks suggests that crustal thickening (i.e. continental collision), and the interleaving of lithologies from the Glenburgh Terrane and Yilgarn Craton occurred during the latter part of the Glenburgh Orogeny, at 1965–1950 Ma (Johnson et al., 2010b). However, since most lithological contacts in the Errabiddy Shear Zone are tectonic, it has yet to be demonstrated whether the conductive crust of the Glenburgh Terrane could represent the reworked margin of the Yilgarn Craton, which had been the site for the addition of voluminous 2555–2430 Ma material.

The Yilgarn Craton is divided into several terranes and domains based on recent geological mapping and a re-evaluation of geological data at various scales (Cassidy et al., 2006). In the northern Yilgarn Craton, these include the Narryer Terrane, the Youanmi Terrane (consisting of the Murchison and Southern Cross Domains), and the Eastern Goldfields Superterrane. The ages and isotopic evolution of various magmatic suites throughout the Yilgarn Craton have been extensively studied, at least in terms of their U–Pb crystallization ages and whole-rock Sm–Nd isotopic compositions, and a vast array of data is available for comparison with the Halfway Gneiss.

The oldest and most distinct terrane is the Narryer Terrane, which contains crust as old as c. 3800 Ma and detrital zircons as old as c. 4400 Ma (Froude et al., 1983; Compston and Pidgeon, 1986; Wilde et al., 2001). The Youanmi Terrane (Murchison and Southern Cross Domains) and the Eastern Goldfields Superterrane are dominated by granite–greenstones with crust as old as c. 3000 Ma (Champion and Cassidy, 2002; Cassidy et al., 2006). The northern Yilgarn terranes were intruded by large volumes of granitic rocks between 2800 and 2600 Ma (Champion and Cassidy, 2002; Cassidy et al., 2006). A comparison of U–Pb crystallization ages of magmatic and inherited zircons derived from granitic rocks and gneisses within the Yarlarweelor Gneiss Complex and Errabiddy Shear Zone (reworked Narryer Terrane and Murchison Domain rocks; Geological Survey of Western Australia, 2009) with those from the Halfway Gneiss is shown in Figure 12. The limited number of >2800 Ma xenocrysts from the Halfway Gneiss makes comparisons with the older parts of the Yilgarn Craton difficult; however, the earliest part of the younger history of the Halfway Gneiss, between 2730 and 2600 Ma, broadly overlaps with magmatism in the northern Yilgarn Craton (Fig. 12). Significantly, there are no magmatic counterparts in the Yilgarn Craton for the younger and larger <2600 Ma event in the Halfway Gneiss (Fig. 12).

All currently available zircon Lu–Hf isotopic data for the Narryer Terrane and Murchison Domain (Griffin et al., 2004; GSWA Geochronology website <www.dmp.wa.gov.au/geochron>) have been assembled into an event signature plot* (Fig. 13). Due to the lack of available zircon Lu–Hf data, especially for the Eastern Goldfields Superterrane and Southern Cross Domain, the plot is supplemented by whole-rock Sm–Nd isotopic data for the granites in these regions (Champion and Cassidy, 2002; GSWA, unpublished data). Two event signatures have been calculated, one for the Narryer Terrane and Murchison Domain in the northwest, and the other for the remainder of the Yilgarn Craton (Fig. 13). Although it is not possible to compare the early history (i.e. older than 2800 Ma) of the terranes, owing to the limited number of data points for the Halfway Gneiss, the 2730–2600 Ma interval is critical, due to the active magmatism in both the Yilgarn Craton and Halfway Gneiss at this time. Apart from a short pulse of juvenile-dominated magmatism in the Narryer Terrane and Murchison Domain at 2830–2800 Ma, the event signature curves for both the Narryer Terrane and Murchison Domain, and the remainder of the Yilgarn Craton, are very similar. From 3000 to 2630 Ma, both curves show near-neutral trends, indicative of mixing between mantle-derived juvenile material with older crustal components (e.g. Van Kranendonk et al., 2010). From 2630 to 2600 Ma, both curves show strongly negative recycling trends without the input of any juvenile material (Van Kranendonk et al., 2010). This contrasts with the upward trend in the curve for the Halfway Gneiss, which is dominated by juvenile processes from 2730 to 2600 Ma. No magmatism younger than 2600 Ma is recorded in the Yilgarn Craton (including the Narryer Terrane and Murchison Domain), whereas the bulk of the Halfway Gneiss formed between 2600 and 2430 Ma.

The apparent coincidence of 2800–2600 Ma magmatism within the northern Yilgarn Craton and the Halfway Gneiss (Fig. 12) is not surprising, because many of Earth's cratonic regions show a similar temporal and isotopic evolution over this period (Condie, 1998; Rino et al., 2004; Condie et al., 2005; Zeh et al., 2009; Iizuka et al., 2010; Hawkesworth et al., 2010). Magmatism during this interval has been related to large-scale mantle overturn events, and is a feature common to most late Archean cratons (e.g. Condie, 1998; Rino et al., 2004). Therefore, the presence of this event in both the Halfway Gneiss and the Yilgarn Craton does not necessarily imply a spatial connection at this time.

In summary, the Halfway Gneiss and Yilgarn Craton record a similar broad period of magmatism between 2800–2600 Ma, a period of activity shared by most Archean cratons worldwide (Condie, 1998; Rino et al., 2004; Condie et al., 2005; Zeh et al., 2009; Iizuka et al., 2010). In contrast to those in the Yilgarn Craton, the 2730–2600 Ma magmatic rocks of the Glenburgh Terrane have a significantly different isotopic evolution, having formed predominantly via juvenile processes. Furthermore, the bulk of the Halfway Gneiss appears to have formed between 2600–2430 Ma, a period of magmatic quiescence

* The Lu–Hf isotopic data presented in Griffin et al. (2004) have been recalculated using the decay constant of Scherer et al. (2001).

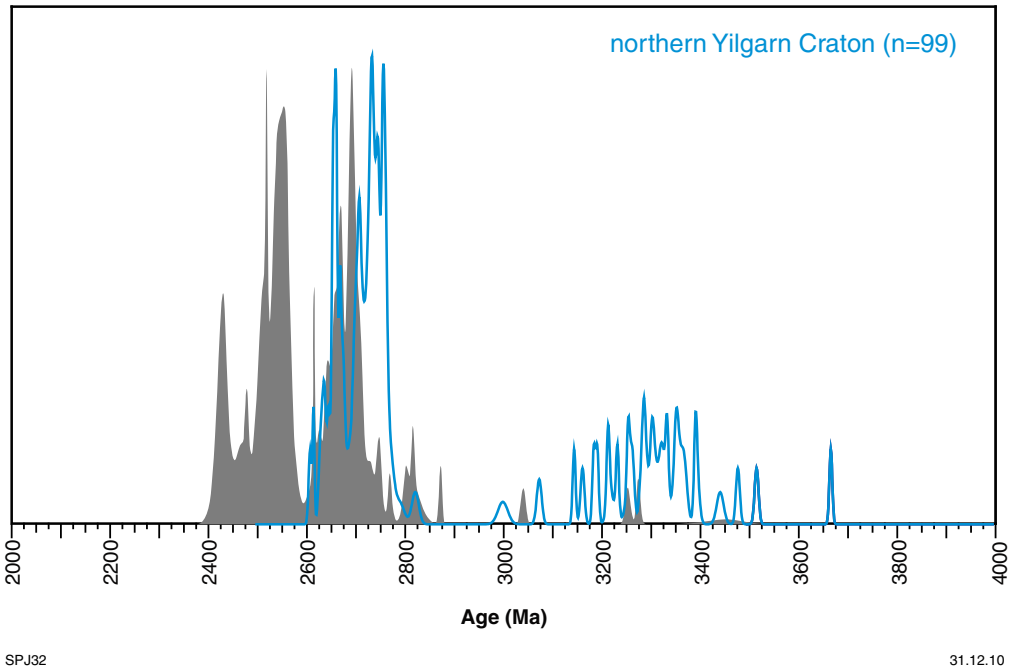

Figure 12. Probability density diagram of zircon ages for Halfway Gneiss samples (this study; grey shaded field) and the northern part of the Yilgarn Craton (blue line; reworked Narryer Terrane and Murchison Domains; Geological Survey of Western Australia, 2009).

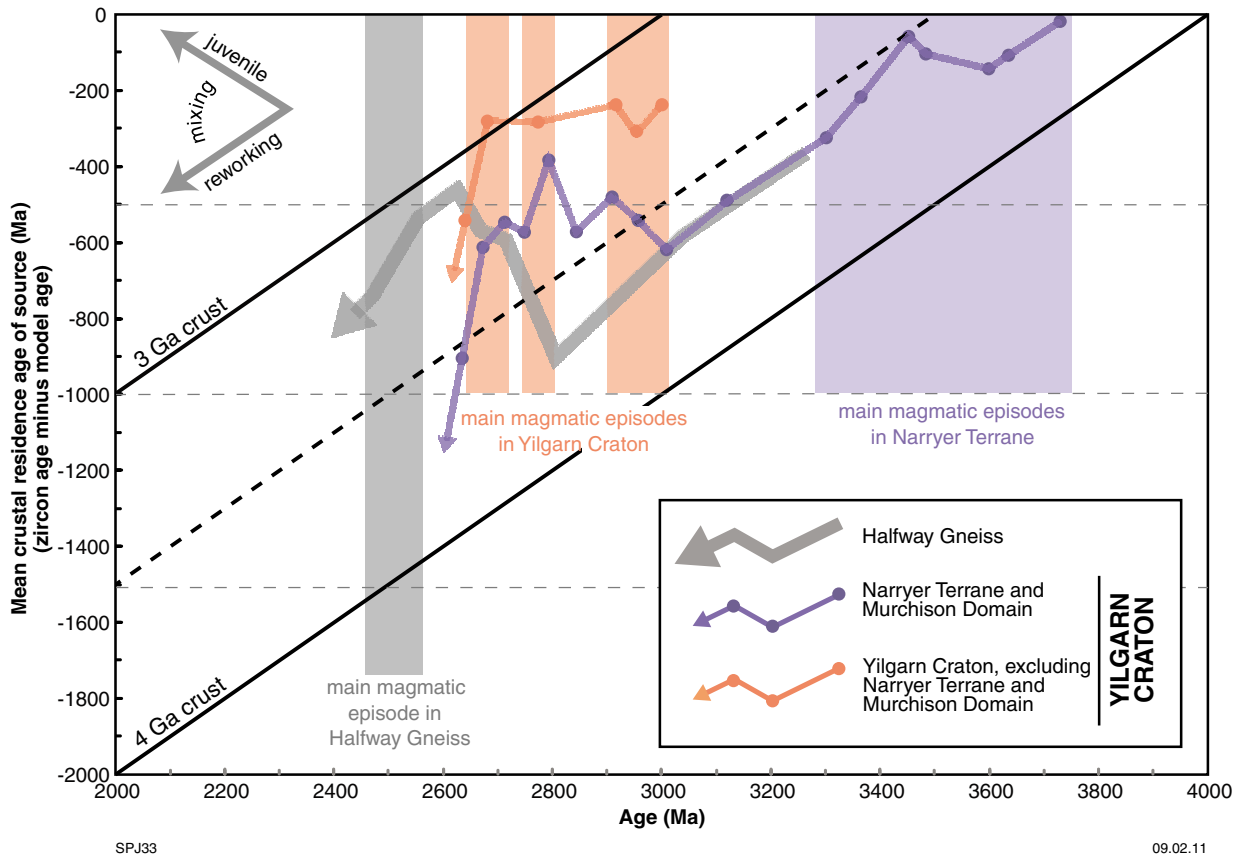

Figure 13. Comparison of event signatures for the Halfway Gneiss, Narryer Terrane and Murchison Domain, and the remainder of the Yilgarn Craton. Age data for the Yilgarn Craton are from Geological Survey of Western Australia (2009); Sm–Nd isotope data are from Champion and Cassidy (2002) and GSWA (unpublished data); Lu–Hf data are from Griffin et al. (2004) and GSWA Geochronology website (<www.dmp.wa.gov.au/geochron>). The event signature curve for the Narryer Terrane and Murchison Domain was constructed using 220 Lu–Hf zircon and Sm–Nd whole-rock analyses, and the curve for the remainder of the Yilgarn Craton was constructed using 191 Sm–Nd whole-rock analyses.

in the Yilgarn Craton. The presence of 2005–1970 Ma Andean-type, subduction-related intrusions of the Dalgaringa Supersuite within the Halfway Gneiss (Kinny et al., 2004; Sheppard et al., 2004), which are also absent from the Yilgarn Craton, indicates that a continental-margin arc was established along the southern margin of the Glenburgh Terrane at this time. The lack of intrusions of similar age in the Yilgarn Craton implies that the north-dipping subduction of oceanic crust occurred under the Glenburgh Terrane (Sheppard et al., 2004; Johnson et al., 2010b), thus placing an oceanic tract of unknown size between the Glenburgh Terrane and Yilgarn Craton directly prior to the 2005–1950 Ma Glenburgh Orogeny. The entire magmatic and isotopic history of the Glenburgh Terrane from 2730 Ma to 1970 Ma is significantly different from that of the Yilgarn Craton, and it is therefore unlikely that the Glenburgh Terrane represents a reworked portion of the Yilgarn Craton margin. The moderately south-dipping Errabiddy Shear Zone most likely represents the collisional suture between the Pilbara Craton – Glenburgh Terrane ('Pilboyne Craton') and the Yilgarn Craton (Johnson et al., 2010b), which formed during the 2005–1950 Ma Glenburgh Orogeny.

Conclusions

The Halfway Gneiss, which forms the basement to the Glenburgh Terrane, has a long history extending back to at least c. 3700 Ma. Although the oldest Glenbugh Terrane crust is not exposed, the isotopic composition of magmatic and inherited zircons in the younger gneissic rocks suggests that this basement must have formed through processes involving juvenile material sometime between 3500 and 2800 Ma. From 2730 to 2600 Ma, renewed crustal growth occurred via the input of significant juvenile (mantle-derived) material, possibly in a suprasubduction setting. Much of the Halfway Gneiss formed between 2600 and 2430 Ma, as recorded by 51% of all dated magmatic and inherited zircons. Crustal evolution occurred by the reworking of older gneiss components, especially those formed during the 2730–2600 Ma episode. This tectono-magmatic history is distinctly different from that recorded in the adjacent Pilbara and Yilgarn Cratons, suggesting that the Glenburgh Terrane is exotic to both these cratons, developing independently prior to their Paleoproterozoic juxtaposition within the West Australian Craton.

These results, together with the findings of Occhipinti et al. (2004), Johnson et al. (2010b), and Sheppard et al. (2010b), demonstrate that the assembly of the West Australian Craton was complete by 1965–1950 Ma, rather than by c. 1800 Ma as initially proposed by Tyler and Thorne (1990). Amalgamation involved three unrelated tectonic blocks during two separate tectonic events. First, the collision or accretion of the Glenburgh Terrane with the Pilbara Craton presumably occurred during the 2215–2145 Ma Ophthalmian Orogeny. A combined Pilbara–Glenburgh block, informally known as the 'Pilboyne Craton', then collided with the Yilgarn Craton during the 1965–1950 Ma Glenburgh Orogeny. Subsequent deformation, metamorphism, and magmatism associated with the 1820–1770 Ma Capricorn Orogeny, 1680–1620 Ma Mangaroon Orogeny, and 1030–955 Ma Edmundian Orogeny, reflect intraplate reworking within the assembled craton.

References

Abdulah, A 2007, Seismic body wave attenuation tomography beneath the Australasian region: Australian National University, Canberra, Australian Capital Territory, PhD thesis (unpublished).

Arndt, NT, Nelson, DR, Compston, W, Trendall, AF and Thorne, AM 1991, The age of the Fortescue Group, Hamersley Basin, Western Australia, from ion microprobe zircon U–Pb results: Australian Journal of Earth Sciences, v. 38, p. 261–281.

Barley, ME, Pickard, AL and Sylvester, PJ 1997, Emplacement of a large igneous province as a possible cause of banded iron-formation 2.45 billion years ago: Nature, v. 385, p. 55–58.

Belousova, EA, Reid, AJ, Griffin, WL and O'Reilly, SY 2009, Rejuvenation vs. recycling of Archean crust in the Gawler Craton, South Australia: Evidence from U–Pb and Hf isotopes in detrital zircon: Lithos, v. 113, p. 570–582.

Blake, TS and Barley, ME 1992, Tectonic evolution of the Late Archaean to Early Proterozoic Mount Bruce megasequence set, Western Australia: Tectonics, v. 11, p. 1415–1425.

Cassidy, KF, Champion, DC, Krapež, B, Barley, ME, Brown, SJA, Blewett, RS, Groenewald, PB and Tyler, IM 2006, A revised geological framework for the Yilgarn Craton, Western Australia: Geological Survey of Western Australia, Record 2006/8, 8p.

Cawood, PA and Tyler, IM 2004, Assembling and reactivating the Proterozoic Capricorn Orogen: lithotectonic elements, orogenies, and significance: Precambrian Research, v. 128, p. 201–218.

Champion, DC and Cassidy, KF 2002, Granites of the northern Eastern Goldfields: their distribution, age, geochemistry, petrogenesis, relationships with mineralisation, and implications for tectonic environment, *in* The characterisation and metallogenic significance of Archean granitoids in the Yilgarn Craton *edited by* KF Cassidy, DC Champion, NJ McNaughton, IR Fletcher, AJ Whitaker, IA Bastrakova and AR Budd: MERIWA Project M281, Report 222, p. 2.1 – 2.49.

Compston, W and Pidgeon, RT 1986, Jack Hills, evidence of more very old detrital zircons in Western Australia: Nature, v. 321, p. 766–769.

Condie, KC 1998, Episodic continental growth and supercontinents: A mantle avalanche connection?: Earth and Planetary Science Letters, v. 163, no. 1–4, p. 97–108.

Condie, KC, Beyer, E, Belousova, E, Griffin, WL and O'Reilly, SY 2005, U–Pb isotopic ages and Hf isotopic composition of single zircons: The search for juvenile Precambrian continental crust: Precambrian Research, v. 139, no. 1–2, p. 42–100.

Frost, BR, Barnes, CG, Collins, WJ, Arculus, RJ, Ellis, DJ and Frost, CD 2001, A geochemical classification for granitic rocks: Journal of Petrology, v. 42, no. 11, p. 2033–2048.

Froude, DO, Ireland, TR, Kinny, PD, Williams, IS, Compston, W, Williams, IR and Myers, JS 1983, Ion microprobe identification of 4100–4200 Myr-old terrestrial zircons: Nature, v. 304, p. 616–618.

Geological Survey of Western Australia 2009, Compilation of geochronology data, June 2009 update: Geological Survey of Western Australia, digital compilation.

Griffin, WL, Belousova, EA, Shee, SR, Pearson, NJ and O'Reilly, SY 2004, Archean crustal evolution in the northern Yilgarn Craton: U–Pb and Hf-isotope evidence from detrital zircons: Precambrian Research, v. 127, p. 19–41.

Griffin, WL, Belousova, EA, Walters, SG and O'Reilly, SY 2006, Archaean and Proterozoic crustal evolution in the Eastern Succession of the Mt Isa district, Australia: U–Pb and Hf-isotope studies of

detrital zircons: Australian Journal of Earth Sciences, v. 53, no. 1, p. 125–149.

Griffin, WL, Wang, X, Jackson, SE, Pearson, NJ, O'Reilly, SY, Xu, X and Zhou, X 2002, Zircon chemistry and magma genesis, SE China: in-situ analysis of Hf isotopes, Pingtan and Tonglu igneous complexes: Lithos, v. 61, p. 237–269.

Hawkesworth, CJ, Dhuime, B, Pietranik, AB, Cawood, PA, Kemp, AIS and Storey, CD 2010, The generation and evolution of the continental crust: Journal of the Geological Society, v. 167, no. 2, p. 229–248.

Iizuka, T, Komiya, T, Rino, S, Maruyama, S and Hirata, T 2010, Detrital zircon evidence for Hf-isotopic evolution of granitoid crust and continental growth: Geochimica et Cosmochimica Acta, v. 74, no. 8, p. 2450–2472.

Johnson, SP, Sheppard, S, Krapf, CBE and Thorne, AM 2010a, Pink Hills, WA Sheet 2248: Geological Survey of Western Australia, 1:100 000 Geological Series.

Johnson, SP, Sheppard, S, Rasmussen, B, Wingate, MTD, Kirkland, CL, Muhling, JR, Fletcher, IR and Belousova, E 2010b, The Glenburgh Orogeny as a record of Paleoproterozoic continent–continent collision: Geological Survey of Western Australia, Record 2010/5, 54p.

Kinny, PD, Nutman, AP and Occhipinti, SA 2004, Reconnaissance dating of events recorded in the southern part of the Capricorn Orogen: Precambrian Research, v. 128, p. 279–294.

Martin, DM, Li, ZX, Nemchin, AA and Powell, CM 1998, A pre-2.2 Ga age for giant hematite ores of the Hamersley Province, Australia: Economic Geology, v. 93, p. 1084–1090.

Martin, DM and Morris, PA 2010, Tectonic setting and regional implications of ca 2.2 Ga mafic magmatism in the southern Hamersley Province, Western Australia: Australian Journal of Earth Sciences, v. 57, no. 7, p. 911–931.

Martin, DM, Sircombe, KN, Thorne, AM, Cawood, PA and Nemchin, AA 2008, Provenance history of the Bangemall Supergroup and implications for the Mesoproterozoic paleogeography of the West Australian Craton: Precambrian Research, v. 166, no. 1–4 (Assembling Australia: Proterozoic building of a continent), p. 93–110.

Martin, DM and Thorne, AM 2004, Tectonic setting and basin evolution of the Bangemall Supergroup in the northwestern Capricorn Orogen: Precambrian Research, v. 128, p. 385–409.

Müller, SG, Krapež, B, Barley, ME and Fletcher, IR 2005, Giant iron-ore deposits of the Hamersley province related to the breakup of Paleoproterozoic Australia: New insights from in situ SHRIMP dating of baddeleyite from mafic intrusions: Geology, v. 33, no. 7, p. 577–580.

Myers, JS 1990, Precambrian tectonic evolution of part of Gondwana, southwestern Australia: Geology, v. 18, p. 537–540.

Myers, JS, Shaw, RD and Tyler, IM 1996, Tectonic evolution of Proterozoic Australia: Tectonics, v. 15, p. 1431–1146.

Nakamura, N 1974, Determination of REE, Ba, Fe, Mg, Na and K in carbonaceous and ordinary chondrites: Geochimica et Cosmochimica Acta, v. 38, p. 757–775.

Nelson, DR 2000a, 142988: biotite tonalite, Dunnawah Bore; Geochronology Record 291, Geological Survey of Western Australia, 4p.

Nelson, DR 2000b, 164309: foliated porphyritic biotite granodiorite, Middle Well; Geochronology Record 217, Geological Survey of Western Australia, 4p.

Nelson, DR 2001, 168950: pegmatite-banded biotite tonalite gneiss, Yanderra Well; Geochronology Record 188, Geological Survey of Western Australia, 4p.

Occhipinti, SA and Sheppard, S 2000, Glenburgh, WA Sheet 2147: Geological Survey of Western Australia, 1:100 000 Geological Series.

Occhipinti, SA and Sheppard, S 2001, Geology of the Glenburgh 1:100 000 sheet: Geological Survey of Western Australia, 1:100 000 Geological Series Explanatory Notes, 37p.

Occhipinti, SA, Sheppard, S, Passchier, C, Tyler, IM and Nelson, DR 2004, Palaeoproterozoic crustal accretion and collision in the southern Capricorn Orogen: the Glenburgh Orogeny: Precambrian Research, v. 128, p. 237–255.

Pearce, JA, Harris, NBW and Tindle, AG 1984, Trace element discrimination diagrams for the tectonic interpretation of granitic rocks: Journal of Petrology, v. 25, p. 956–983.

Pickard, AL 2002, SHRIMP U–Pb zircon ages of tuffaceous mudrocks in the Brockman Iron Formation of the Hamersley Range, Western Australia: Australian Journal of Earth Sciences, v. 49, no. 3, p. 491–507.

Rasmussen, B, Blake, TS and Fletcher, IR 2005a, U–Pb zircon age constraints on the Hamersley spherule beds: Evidence for a single 2.63 Ga Jeerinah–Carawine impact ejecta layer: Geology, v. 33, no. 9, p. 725–728.

Rasmussen, B and Fletcher, IR 2010, Dating sedimentary rocks using in situ U–Pb geochronology of syneruptive zircon in ash-fall tuffs <1mm thick: Geology, v. 38, no. 4, p. 299–302.

Rasmussen, B, Fletcher, IR and Sheppard, S 2005b, Isotopic dating of the migration of a low-grade metamorphic front during orogenesis: Geology, v. 33, p. 773–776.

Rino, S, Komiya, T, Windley, BF, Katayama, I, Motoki, A and Hirata, T 2004, Major episodic increases of continental crustal growth determined from zircon ages of river sands: implications for mantle overturns in the Early Precambrian: Physics of the Earth and Planetary Interiors, v. 146, no. 1–2, p. 369–394.

Scherer, E, Münker, C and Mezger, K 2001, Calibration of the lutetium–hafnium clock: Science, v. 293, p. 683–687.

Selway, K 2008, Magnetotelluric investigation into the electrical structure of the Capricorn Orogen, Western Australia: Geological Survey of Western Australia, Record 2007/16, 39p.

Selway, K, Sheppard, S, Thorne, AM, Johnson, SP and Groenewald, PB 2009, Identifying the lithospheric structure of a Precambrian orogen using magnetotellurics: the Capricorn Orogen, Western Australia: Precambrian Research, v. 168, p. 185–196.

Sheppard, S 2005, Does the ca.01800 Ma Capricorn Orogeny mark collision of the Yilgarn and Pilbara Cratons? *edited by* MTD Wingate and SA Pisarevsky: Geological Society of Australia; Supercontinents and Earth Evolution Symposium 2005, Fremantle, Western Australia, 26 October 2005, p. 29.

Sheppard, S, Bodorkos, S, Johnson, SP, Wingate, MTD and Kirkland, CL 2010a, The Paleoproterozoic Capricorn Orogeny: intracontinental reworking not continent–continent collision: Geological Survey of Western Australia, Report 108, 33p.

Sheppard, S, Johnson, SP, Groenewald, PB and Farrell, TR 2008, Yinnetharra, WA Sheet 2148: Geological Survey of Western Australia, 1:100 000 Geological Series.

Sheppard, S, Johnson, SP, Wingate, MTD, Kirkland, CL and Pirajno, F 2010b, Explanatory Notes for the Gascoyne Province: Geological Survey of Western Australia, Perth, Western Australia, 336p.

Sheppard, S, Occhipinti, SA and Tyler, IM 2004, A 2005–1970 Ma Andean-type batholith in the southern Gascoyne Complex, Western Australia: Precambrian Research, v. 128 (Assembling the Palaeoproterozoic Capricorn Orogen), p. 257–277.

Thorne, AM, Martin, DM, Johnson, SP, Sheppard, S and Cutten, HN 2010, Candolle, WA Sheet 2348 (2nd edition): Geological Survey of Western Australia, 1:100 000 Geological Series.

Thorne, AM and Seymour, DB 1991, Geology of the Ashburton Basin, Western Australia: Geological Survey of Western Australia, Bulletin 139, 141p.

Trendall, AF 1975, Precambrian: introduction, in Geology of Western Australia: Geological Survey of Western Australia, Memoir 2, p. 25–32.

Trendall, AF, Compston, W, Nelson, DR, de Laeter, JR and Bennett, VC 2004, SHRIMP zircon ages constraining the depositional chronology of the Hamersley Group, Western Australia: Australian Journal of Earth Sciences, v. 51, no. 5, p. 621–644.

Trendall, AF, Nelson, DR, de Laeter, JR and Hassler, SW 1998, Precise zircon U–Pb ages from the Marra Mamba Iron Formation and Wittenoom Formation, Hamersley Group, Western Australia: Australian Journal of Earth Sciences, v. 45, p. 137–142.

Tyler, IM and Thorne, AM 1990, The northern margin of the Capricorn Orogen, Western Australia — an example of an early Proterozoic collision zone: Journal of Structural Geology, v. 12, p. 685–701.

Van Kranendonk, MJ, Ivanic, TJ, Wingate, MTD and Kirkland, CL 2010, Long lived, autochthonous development of the Murchison Domain, Yilgarn Craton, in Earth systems: change, sustainability, vulnerability: Geological Society of Australia; Australian Earth Sciences Convention 2010, Canberra, 4 July 2010, p. 130.

Van Kranendonk, MJ, Smithies, RH, Hickman, AH and Champion, DC 2007, Review: secular tectonic evolution of Archean continental crust: interplay between horizontal and vertical processes in the formation of the Pilbara Craton, Australia: Terra Nova, v. 19, no. 1, p. 1–38.

Wilde, SA, Valley, JW, Peck, WH and Graham, CM 2001, Evidence from detrital zircons for the existence of continental crust and oceans on the Earth 4.4 Gyr ago: Nature, v. 409, p. 175–178.

Williams, SJ 1986, Geology of the Gascoyne Province, Western Australia: Geological Survey of Western Australia, Report 15, 85p.

Wingate, MTD, Kirkland, CL, Sheppard, S and Johnson, SP 2010, 185955: leucocratic granitic gneiss, Wabli Creek; Geochronology Record 908, Geological Survey of Western Australia, 4p.

Zeh, A, Gerdes, A and Barton Jr, JM 2009, Archean accretion and crustal evolution of the Kalahari Craton — the zircon age and Hf isotope record of granitic rocks from Barberton/Swaziland to the Francistown Arc: Journal of Petrology, v. 50, no. 5, p. 933–966.

Appendix 1

Zircon Lu–Hf isotope analyses

Hf-isotope analyses were carried out using a New Wave/Merchantek LUV213 laser-ablation microprobe, attached to a Nu Plasma multi-collector ICP-MS. The analyses were conducted using a beam diameter of ~55 μm and a 5 Hz repetition rate. Typical ablation times were 100–120 seconds, resulting in pits 40–60 μm deep. Helium carrier gas transported the ablated sample from the laser-ablation cell to the ICP-MS torch via a mixing chamber.

The interference of ^{176}Lu on ^{176}Hf measurements was corrected by measuring the intensity of the interference-free ^{175}Lu isotope and using a ^{176}Lu/^{175}Lu ratio of 1/40.02669 (DeBievre and Taylor, 1993) to calculate ^{176}Lu/^{177}Hf. Similarly, the interference of ^{176}Yb on the measurement of ^{176}Hf was corrected by measuring the interference-free ^{172}Yb isotope and using ^{176}Yb/^{172}Yb to calculate ^{176}Yb/^{177}Hf. The appropriate value of ^{176}Yb/^{172}Yb was determined by spiking the JMC475 Hf standard with ytterbium, and finding the value of ^{176}Yb/^{172}Yb (0.58669) required to yield the ^{176}Hf/^{177}Hf value obtained for the pure hafnium solution. Analyses of standard zircons (Griffin et al., 2000, 2004) illustrate the precision and accuracy obtainable for the ^{176}Hf/^{177}Hf ratio, despite the corrections on ^{176}Hf. The typical 2σ precision of ^{176}Hf/^{177}Hf ratios is +0.00002, equivalent to +0.7 εHf unit. The accuracy and precision of the method were discussed in detail by Griffin et al. (2000, 2004) and interference corrections for ^{176}Lu and ^{176}Yb were described by Griffin et al. (2006, 2007).

The Mud Tank zircon standard, analysed after every ten unknown zircons, was used as an independent control on reproducibility and instrument stability. Most of the data and the mean value (0.282527 ± 28; n = 10) are within 2 s.d. of the recommended values (0.282522 ± 42 (2σ); Griffin et al., 2007). A single analysis of the 91500 zircon standard analysed during this study yielded ^{176}Hf/^{177}Hf = 0.282304 ± 42 (2σ), which is well within the range of values reported for this standard (Griffin et al., 2006).

For calculation of εHf values, the chondritic values of Scherer et al. (2001) were adopted. To calculate model ages (T_{DM}) based on a depleted-mantle source, a model with (^{176}Hf/^{177}Hf)i = 0.279718 at 4.56 Ga and ^{176}Lu/^{177}Hf = 0.0384 were used; this produces a present-day value of ^{176}Hf/^{177}Hf (0.28325), similar to that of average MORB (Griffin et al., 2000, 2004). T_{DM} ages, calculated using the measured ^{176}Lu/^{177}Hf of the zircon, can only give a minimum age for the source material of the magma from which the zircon crystallized. Therefore, also calculated for each zircon is a 'crustal' model age that assumes its parental magma was produced from a volume of average continental crust with a ^{176}Lu/^{177}Hf ratio of 0.015 (Griffin et al., 2002).

References

DeBievre, P and Taylor, PDP 1993, Table of the isotopic composition of the elements: International Journal of Mass Spectrometry and Ion Processes, v. 123, p. 149.

Griffin, WL, Belousova, EA, Shee, SR, Pearson, NJ and O'Reilly, SY 2004, Archean crustal evolution in the northern Yilgarn Craton: U–Pb and Hf-isotope evidence from detrital zircons: Precambrian Research, v. 127, p. 19–41.

Griffin, WL, Pearson, NJ, Belousova, EA, Jackson, SE, O'Reilly, SY, van Achterberg, E and Shee, SR 2000, The Hf isotope composition of cratonic mantle: LAM-MC-ICPMS analysis of zircon megacrysts in kimberlites: Geochimica et Cosmochimica Acta, v. 64, p. 133–147.

Griffin, WL, Pearson, NJ, Belousova, EA and Saeed, A 2006, Comment: Hf-isotope heterogeneity in standard zircon 91500: Chemical Geology, v. 233, p. 358–363.

Griffin, WL, Pearson, NJ, Belousova, EA and Saeed, A 2007, Reply to 'Comment to short-communication 'Comment: Hf-isotope heterogeneity in zircon 91500' by WL Griffin, NJ Pearson, EA Belousova, A Saeed (Chemical Geology 233 (2006) p. 358–363)' *by* F Corfu: Chemical Geology, v. 244, p. 354–356.

Griffin, WL, Wang, X, Jackson, SE, Pearson, NJ, O'Reilly, SY, Xu, X and Zhou, X 2002, Zircon chemistry and magma genesis, SE China: in-situ analysis of Hf isotopes, Pingtan and Tonglu igneous complexes: Lithos, v. 61, p. 237–269.

Scherer, E, Münker, C and Mezger, K 2001, Calibration of the lutetium–hafnium clock: Science, v. 293, p. 683–687.

This report details the geological and isotopic evolution of the Halfway Gneiss, the oldest part of the Glenburgh Terrane, which forms basement to the entire Gascoyne Province. Secondary ion mass spectrometry (SIMS) zircon dating, combined with in situ lutetium–hafnium isotope analyses of zircons, reveal a long and punctuated crustal history ranging back to 3700 Ma, with major periods of crustal growth at 2730–2600 and 2555–2430 Ma.
The geochronological and isotopic evolution of the Halfway Gneiss is unlike that of the bounding Pilbara and Yilgarn Cratons, indicating that the Glenburgh Terrane was an exotic piece of crust prior to amalgamation of the West Australian Craton.

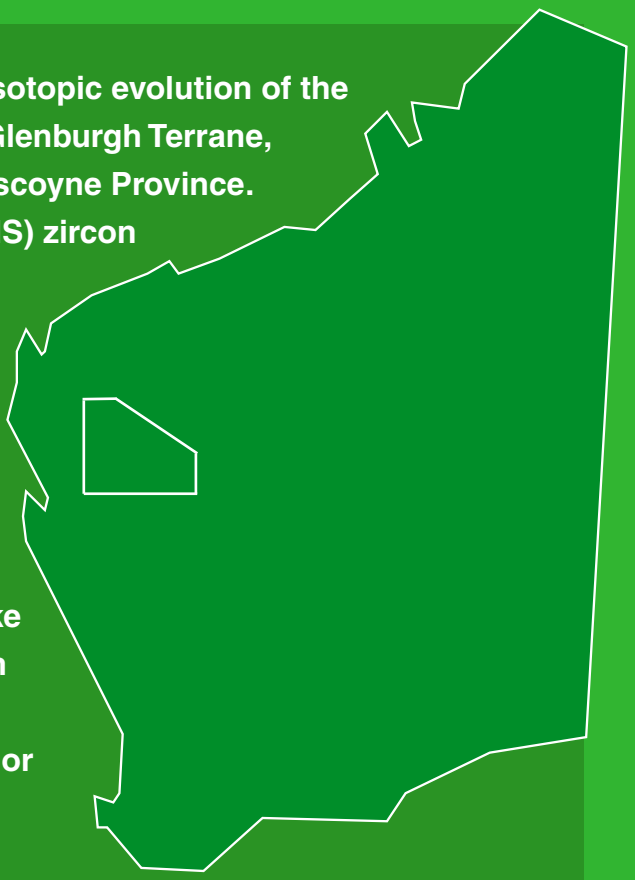

Johnson et al.

Temporal and hafnium isotopic evolution of the Glenburgh Terrane basement: an exotic crustal fragment in the Capricorn Orogen

REPORT 110

Further details of geological publications and maps produced by the Geological Survey of Western Australia are available from:

Information Centre
Department of Mines and Petroleum
100 Plain Street
East Perth WA 6004
Phone: (08) 9222 3459 Fax: (08) 9222 3444
<http://www.dmp.wa.gov.au/GSWApublications>